# Development of Si-O-C Based Ceramic Matrix Composites Produced via Pyrolysis of a Polysiloxane

**By**

**Hatice Deniz AKKAŞ**

**A Dissertation Submitted to the
Graduate School in Partial Fulfillment of the
Requirements for the Degree of**

## MASTER OF SCIENCE

**Department: Materials Science and Engineering
Major: Materials Science**

**İzmir Institute of Technology
İzmir, Turkey**

**July, 2004**

We approve the thesis of **Hatice Deniz Akkaş**

Date of Signature

---------- **29.07.2004**

**Assoc. Prof. Dr. Metin Tanoğlu**

Supervisor

Department of Mechanical Engineering

---------- **29.07.2004**

**Prof. Dr. Muhsin Çiftçioğlu**

Department of Chemical Engineering

---------- **29.07.2004**

**Assoc. Prof. Dr. Funda Tıhmınlıoğlu**

Department of Chemical Engineering

---------- **29.07.2004**

**Prof. Dr. Muhsin Çiftçioğlu**

Head of Department

# ACKNOWLEDGEMENTS

I wish to express my sincere gratitude to my advisors Assoc. Prof. Metin Tanoğlu and Prof. M. Lütfi Öveçoğlu for their supervisions, guidance, encouragement and supports during the course of this thesis and in the experimental study. I acknowledge the supports of The Scientific and Technical Research Council of Turkey (TÜBİTAK) for the financial support for MİSAG 215 project. Finally, I would like to thank my family for their understanding, encouragement and supports.

# ABSTRACT

The traditional ceramic processing techniques of CMCs such as hot pressing are high-temperature, high-cost processes, and unsuitable for manufacturing complex and near-net shapes. Fabrication of ceramic matrix composites (CMCs) from pyrolytic conversion of preceramic polymers has gained considerable attention in recent years due to their unique combination of low temperature processing, applicability of versatile plastic shaping technologies and microstructural control capabilities.

In the present work, phenyl (PPS) and methyl (PMS) containing polysiloxanes were pyrolyzed at elevated temperatures (900-1500$^{o}$C) without filler addition under argon atmosphere to investigate the thermal conversions and phase formations in the polymer matrix. X-Ray diffraction (XRD) and Infrared spectroscopy (FTIR) techniques were used for this purpose. It was found that pyrolysis of the polymers under inert atmosphere up to 1300$^{o}$C lead to amorphous silicon oxycarbide ($SiO_xC_y$) ceramics. Conversions at higher temperatures caused the transformation into the crystalline β-SiC phases. % Weight changes of the samples without filler addition were also followed by measuring the masses before and after pyrolyzation of the samples.

CMC monoliths were fabricated with the addition of 60-80 wt% active and inert fillers by hot pressing under 15 MPa pressure and pyrolysis at elevated temperatures between 900-1500$^{o}$C under inert argon and reactive nitrogen atmosphere. Effects of the filler type and ratio, pyrolysis temperature and atmosphere on the phase formations were investigated by using XRD, SEM-EDX and TGA techniques. The results showed that with the incorporation of active Ti fillers, formation of TiC, TiSi, and TiO within the amorphous matrix occurred due to the reactions between the Ti and the polymer decomposition products. However, no new phase development was observed in the case of inert SiC particulate addition. SEM-EDX analysis was also performed to monitor the new phase formations. Mass loss and densification values of the CMCs were measured to investigate the effect of active filler controlled polymer pyrolysis process (AFCOP). Weight changes were considerably affected in the case of addition of the fillers into the ceramic structure due to the reduction of the polymer ratio in the composite systems and the reactions between polymer and filler particles. As an example weight loss of 27 % was measured for PPS samples without filler addition, while 17 % weight reduction was measured for PMS without filler addition after pyrolysis at 1500$^{o}$C. On the other hand,

it was found that for the composite systems the weight loss values were reduced to 2 %. Mechanical property characterization of samples with and without filler addition was done by Vickers Indentation tests. It was found that ceramics that is the product of the pyrolysis of the polymer without filler addition exhibited the maximum hardness values (8.88 GPa for neat PPS, 10.67 GPa for neat PMS) at 1100$^{o}$C, which is the optimum temperature for crack free samples with the least amount of porosity. Also, the composite system exhibited the hardness values up to 14 GPa.

# ÖZ

Sıcak preseme gibi seramik matriks kompozitlerin (CMC) geleneksel üretim yöntemleri, yüksek sıcaklık gerektiren yüksek maliyetli yöntemlerdir ve kompleks ve son net şekle benzer yapıların üretimi için uygun değillerdir. CMClerin önseramik polimerlerin pirolitik dönüşümü ile üretimleri, son zamanlarda, düşük sıcaklık, çok yönlü plastik şekillendirme yöntemlerinin uygulanabilirliği ve mikroyapısal kontrol kolaylığı gibi özgün kombinasyonlarına bağlı olarak artan bir önem kazanmıştır.

Bu çalışmada, fenil (PPS) ve metil (PMS) ihtiva eden polisiloksanlar polimerlerin ısıl dönüşümleri ve faz oluşumlarının incelenmesi için dolgu malzemesi ilave edilmeden, artan piroliz sıcaklıklarında (900-1500$^{o}$C) ve argon atmosferinde üretilmiştir. Bu amaç için X-ışınları kırınımı (XRD) ve kızılötesi spektroskopisi (FTIR) yöntemleri kullanılmıştır. Bunun sonucunda, inert atmosferde 1300$^{o}$C'ye kadar gerçekleşen pirolizin amorf silikon oksikarbür ($SiO_xC_y$) seramiklerine yol açtığı gözlenmiştir. Daha yüksek sıcaklıklardaki dönüşüm β-SiC kristallerinin oluşumuna sebep olmuştur. Piroliz öncesi ve sonrası kütlelerin ölçülmesi ile % ağırlık değişimleri takip edilmiştir.

CMC kompozitler ağırlıkça % 60-80 arasında değişen aktif ve inert dolgular ilave edilerek 15 MPa basınçta sıcak preslemeyle üretilmiş ve inert argon ve reaktif azot atmosferinde 900-1500$^{o}$C arasındaki sıcaklıklarda piroliz edilmişlerdir. Dolgu tipi ve oranının, piroliz sıcaklığı ve atmosferin faz oluşumlarına etkileri XRD, SEM-EDX ve TGA yöntemleriyle incelenmiştir. Sonuçlar göstermiştir ki, Ti gibi aktif bir dolgu maddesinin kullanılması sonucu bunun polimerin bozunma ürünleri ile reaksiyonuna bağlı olarak amorf matriks içerisinde TiC, TiSi, ve TiO oluşmuştur. Ancak inert SiC ilavesi durumunda yeni faz oluşumu gözlenmemiştir. SEM-EDX analizleri bu faz oluşumlarının saptanmasında kullanılmıştır. Aktif dolgu kontrollü polimer piroliz (AFCOP) tekniğinin etkilerini incelemek için CMClerin kütle kaybı ve yoğunluk artışı değerleri ölçülmüştü. Kütle değişimleri seramik yapılara dolgu ilave edilerek polimer oranının düşmesi ve dolgu malzemesi ile polimer arasındaki reaksiyonlara bağlı olarak belirgin şekilde etkilenmiştir. Dolgusuz PPS örnekleri için % 27'lik, dolgusuz PMS için ise % 17'lik bir kütle kaybı 1500$^{o}$C'de pirolizlenen örneklerde ölçülmüştür. Diğer yandan kompozit sistemlerinde bu değerin % 2'lere kadar düştüğü görülmüştür. Kütle değişimlerinin ölçülmesinde ısıl analiz yöntemleri (TGA) de kullanılmıştır. Katkısız ve

dolgu ilave edilmiş örneklerin mekanik karakterizasyonları Vickers Sertlik testleri ile yapılmıştır. Bunun sonucunda, dolgusuz seramikler maksimum sertlik değerlerine (dolgusuz PPS için 8.88 GPa, dolgusuz PMS için 10.67 GPa) çatlaksız ve en az gözenek içeren örneklerin üretildiği optimum sıcaklık olan 1100$^{o}$C'de ulaşılmıştır. Kompozit sistemlerde ise sertlik değerleri 14 GPa kadar çıkmıştır.

# TABLE OF CONTENTS

# LIST OF FIGURES

# LIST OF TABLES

# CHAPTER 1

# INTRODUCTION

There is a great interest for low cost, low temperature (<1000$^{o}$C), near-net-shape ceramic-matrix-composites (CMCs). The traditional processing techniques of CMCs such as hot pressing are high-temperature, high-cost processes, and unsuitable for manufacturing complex and near-net-shapes. Ceramic and CMC manufacturing from pyrolytic conversion of preceramic polymers has gained considerable attention in recent years due to their unique combination of low temperature processing, applicability of versatile plastic shaping technologies and microstructural control capabilities. These materials have potential applications such as lightweight high temperature structural materials, fibers, catalyst supports, and anodes in lithium ion rechargeable batteries.

Poly(silanes), -(carbosilanes), -(silazanes) and -(siloxanes) have been the most studied preceramic precursors because of their commercial availability and high ceramic yields. Silicon oxycarbide glasses that contain silicon atoms bonded to oxygen and carbon randomly are a group of materials that can be produced by pyrolysis of some specific preceramic precursors. The replacement of part of the divalent oxygen atoms of silica by tetravalent carbon atoms leads to an improvement in the thermomechanical properties [1-4]. Substitution of oxygen in silica glass with carbon is not feasible through conventional glass melting techniques due to their high processing temperatures (1600-1800$^{o}$C). However, it may be obtained via pyrolysis of the preceramic polymers [3].

Main drawback of the polymer pyrolysis technique is the manufacturing of crack free bulk ceramic components. Due to inherent density increase by outgassing of the organic matter, extensive shrinkage that causes the formation of pores and cracks may occur. To compensate this effect and to control shrinkage and crack formation, a relatively new concept, active filler controlled polymer pyrolysis process (AFCOP) has been developed [5-7]. This concept became a scope of many other researches, recently [3, 8-11]. According to this method, the polymer is partially filled with inert or active powder particles in order to decrease the shrinkage and to allow the fabrication of bulk, crack free ceramics. By incorporation of the active fillers, reaction between the particles and the precursor occurs, which typically results in a volume expansion of the reaction product, as compared to the starting compounds. This expansion counteracts the

shrinkage during densification and can lead to near-net shaped crack-free components. Suitable active fillers are elements or compounds such as Al, B, Si, Ti, $CrSi_2$, $MoSi_2$, etc. to obtain carbide, nitride or oxide reaction products.

The objective of the present study is to develop ceramic composites from the pyrolysis of two preceramic polymers; poly(phenyl)siloxane and poly(methyl)siloxane with the addition of the active (Ti) and inert (SiC) fillers. Another objective is to investigate the effect of polymer and filler type, filler concentration and pyrolysis temperature on the microstructure, phase development, densification, mass losses and hardness values of the composites.

In the present work, phenyl and methyl containing siloxanes were pyrolyzed without filler addition under argon atmosphere at temperatures between 900-1500$^{o}$C and thermal conversions and phase formations of the samples was monitored using X-Ray diffraction and infrared spectroscopy techniques. Microstructural features of the neat samples were investigated using SEM micrograph coupled with EDX analyzer. Weight changes of the neat samples were followed by measuring the masses before and after pyrolysation of the samples. CMC composite monoliths were also fabricated with the addition of 60-80 wt % active and inert fillers by hot pressing under 15 MPa pressure and pyrolysis at elevated temperatures between 900-1500$^{o}$C under inert argon and reactive nitrogen atmospheres. Effects of filler type and weight fraction, pyrolysis temperature and atmosphere on the phase formations were investigated. SEM-EDX analysis was also performed to monitor the new phase formations. Mass losses and densification behavior of the CMCs were measured to investigate the effect of AFCOP. Thermal Analysis (TGA) was also performed for measuring the mass changes of the samples. Mechanical characterization of the samples with and without filler addition was done by Vickers Indentation tests.

# CHAPTER 2

# CERAMICS

The term “ceramic” comes from the Greek word *keramikos*, which means “burnt earth”, indicating that desirable properties of these materials are normally achieved through a high temperature heat treatment process called firing. Most ceramics are compounds between metallic and nonmetallic elements for which the interatomic bonds are either totally ionic or predominantly ionic but having some covalent character. Up until the past 40 or so years, the most important materials in this class were termed the “traditional ceramics”, those for which the primary raw material is clay; products considered to be traditional ceramics are china, porcelain, bricks, tiles, and, in addition, glasses and high temperature ceramics. Of late, significant progress has been made in understanding the fundamental character of these materials and of the phenomena that occur in them that are responsible for their unique properties. Consequently, a new generation of these materials has evolved, and the term “ceramic” has taken on a much broader meaning [12].

## 2.1 Advanced Ceramics

The new and emerging family of ceramics are referred to as advanced, new or fine, and utilize highly refined materials, often using new forming techniques, special firing treatments, and frequently requiring extensive finishing and testing before being placed in use [13]. These “new” or “advanced” ceramics, when used as an engineering material, posses several properties which can be viewed as superior to metal-based systems that are listed in Table 2.1.

The advance of ceramics technology drew on experience from metallurgical technologies. In the nineteenth and twentieth centuries, there appeared in the marketplace a wide variety of new types of building materials with superior durability, strength, and other properties. These included brick, tile piping for drainage systems and roofing, sanitary ware and refractory (high-temperature) insulation materials which served as furnace linings for glass, steel, and other industries dependant on high-temperature processing of new materials. There are many combinations of metallic and

nonmetallic atoms that can combine to form ceramic components, and also several structural arrangements are usually possible for each combination of atoms. This led scientists to invent many new ceramic materials to meet increasing requirements and demands in various application areas [14].

A relative new comer to advanced ceramics category of materials is the ceramic-matrix-composites (also called CMCs). The use of ceramic reinforcements in polymer-matrix and metal-matrix composites has become fairly common; however, the formation of a composite that uses a ceramic material as the matrix (most often with ceramic fibers, whiskers, or platelets as the reinforcement) is a promising new area of development [13].

**Table 2.1** Comparison of ceramics and metals [43].

| | **Ceramics** | | | | **Comperison materials** | | |
|---|---|---|---|---|---|---|---|
| **Properties** | **Alumina** | **Beryllia** | **Silicon Carbide** | **Zirconia** | **Mild Steel** | **Aluminum** | **Nylon** |
| **Melting point (approximately $^{o}$C)** | 2050 | 2550 | 2800 | 2662 | 1370 | 660.2 | 215 |
| **Coefficient of thermal expansion (m/m/k)x$10^{6}$** | 8.1 | 10.4 | 4.3 | 6.6 | 14.9 | 24 | 90 |
| **Specific gravity** | 3.8 | - | 3.2 | - | 7.9 | 2.7 | 1.15 |
| **Density (kg/m$^{3}$)** | 3875 | 2989 | 3210 | 9965 | 7833 | 2923 | 1163 |
| **Dielectric strength (V/m)x$10^{6}$** | 11.8 | - | - | 9.8 | - | - | 18.5 |
| **Modulus of elasticity (MPa)x$10^{4}$** | 34.5 | 39.9 | 65.5 | 24.1 | 17.2 | 6.9 | 0.33 |
| **Hardness (Mohs)** | 9 | 9 | 9 | 8 | 5 | 3 | 2 |
| **Maximum service temperature (K)** | 2222 | 2672 | 2589 | 2672 | - | - | 442 |

### 2.1.1 Properties of Advanced Ceramics

Advanced materials are recognized to be crucial to the growth, prosperity, and sustained profit-ability of any industry. The National Research Council in the USA investigated eight major US industries that employed seven million people and had sales of 1.4 trillion US dollars in 1987, to examine the role of materials in future technology strategies. The result shows a generic need for lighter, stronger, more corrosion-resistant

materials capable of withstanding high temperatures. Ceramic materials are the leading candidates for meeting these requirements.

There has been great interest shown in advanced or high technology ceramic materials among scientists, policymakers, and corporations in recent years. Varieties of ceramic materials, which hold remarkable properties able to meet the need for high end applications, have appeared. In general terms, advanced ceramics exhibit exceptional properties that make them highly resistant to melting, bending, stretching, corrosion or wear. Their hardness, physical stability, high mechanical strength at high temperature, stiffness, low density, optical conductivity, radiation resistance, extreme heat resistance, chemical inertness, biocompatibility, superior electrical properties and, not least, their stability for use in mass produced products make them one of the most versatile groups of materials in the world. [15] Today, there are a wide range of advanced ceramics including oxides, carbides, nitrides, borides, silicates and glass ceramics and composite (ceramic matrix (CMC), and carbon-carbon (CCC)) materials. The most commonly used are alumina, zirconia, silicon nitride, silicon carbide, steatite, cordierite and many more –each with their own particular performance characteristic and benefits. New materials are being developed all the time in response to the challenges posed by new and changing applications [14].

### 2.1.2 Types of Advanced Ceramic Materials

Alumina is the most widely used advanced ceramic material. It offers very good performance in terms of wear resistance, corrosion resistance and strength at a reasonable price. Its high dielectric properties are beneficial in electronic products. Silicon nitride exceeds other ceramic materials in thermal shock resistance. It also offers an excellent combination of low density, high strength, low thermal expansion and good corrosion resistance and fracture toughness. Silicon carbide has the highest corrosion resistance of all the advanced ceramic materials. It also retains its strength at temperatures as high as 1400°C and offers excellent wear resistance and thermal shock resistance. Zirconia has the highest strength and toughness at room temperature of all the advanced ceramic materials. The fine grain size allows for extremely smooth surfaces and sharp edges [16]. Single crystal sapphire offers superior mechanical properties and chemical stability coupled with light transmission [42]. Some specifications of these materials can be seen in Table 2.2.

**Table 2.2** Properties of some advanced ceramics produced in Kyocera Industrial Ceramic Corporation [42].

| **Material** | | | **Silicon Nitride** ($Si_3N_4$) | | **Silicon Carbide** (SiC) | | **Zirconia** ($ZrO_2$ | **Alumina** ($Al_2O_3$) | | | | **Aluminum Nitride** AlN | |
|---|---|---|---|---|---|---|---|---|---|---|---|---|---|
| **Kyocera No.** | | | SN-220 | SN-235P | SC-211 | SC-1000 | Z-201N | A-479 | A-479G | 99.9% Alumina | 99.95% Alumina | AN2000 | AN2170 |
| **Color** | | | Black | Gray | Black | Black | Ivory | 99% White | 99.5% Ivory | 99.9% Ivory | 99.95% white | Ivory | Brown |
| **Bulk Density** | | — | 3.2 | 3.2 | 3.2 | 3.16 | 6.0 | 3.8 | 3.8 | 3.95 | 3.95 | 3.2 | 3.4 |
| **Water Absorption** | | % | 0 | 0 | 0 | 0 | 0 | 0 | 0 | 0 | 0 | 0 | 0 |
| **Vickers Hardness Load 500g** | | GPa | 13.7 | 14.2 | 23.5 | 24.0 | 12.3 | 16.2 | 17.6 | 17.6 | 20.6 | 10.0 | 10.0 |
| **Flexural Strength (4-point Bending *3-point Bending)** | **R.T.** | $kg/mm^2$ MPa | 60 590 | 69 676 | 55 539 | 49 480 | 100 *980 | 31 *304 | 33 *323 | 50 *490 | 60 *588 | 27 267 | 35 343 |
| | **800°** | $kg/mm^2$ MPa | 61 600 | 69 676 | — | — | 42 *412 | 28 *274 | — | — | — | 25 246 | — |
| | **1000°** | $kg/mm^2$ MPa | 52 510 | 60 600 | 48 470 | 49 480 | 28 *274 | 18 *176 | — | — | — | 24 235 | — |
| | **1200°** | $kg/mm^2$ MPa | 33 323 | 40 392 | 40 392 | 49 480 | 17 *167 | — | — | — | — | 21 208 | — |
| | **1300°** | $kg/mm^2$ MPa | 12 117 | — | — | — | — | — | — | — | — | — | — |
| | **1400°** | $kg/mm^2$ MPa | — | — | 36 353 | 49 480 | — | — | — | — | — | — | — |
| **Fracture Toughness ($K_{1C}$)M.I** | | MPa√m | 5.7 | 5.9 | 5.6 | — | 6.7 | — | — | — | — | 3.1 | 1.8 |
| **Young's Modulus R.T.** | | $x10^6$psi GPa | 43 294 | 43 294 | 63 431 | 63 430 | 30 206 | 50 343 | 53 363 | 56 391 | 56 391 | 43 298 | 44 304 |
| **Poisson's Ratio R.T.** | | — | 0.28 | 0.28 | 0.16 | 0.17 | 0.31 | 0.25 | 0.23 | 0.23 | 0.23 | 0.24 | 0.24 |
| **Coefficient of Linear Thermal Expansion** | **40-400°C** | ($x10^6$/°C | 2.6 | 2.6 | 4.0 | 3.9 | 10.5 | 7.1 | 7.1 | — | — | 5.0 | 4.8 |
| | **40-800°C** | | 3.2 | 3.1 | 4.4 | 4.5 | 11.0 | 7.9 | 7.9 | — | — | — | 5.4 |
| **Thermal Conductivity R.T.** | | cal/cm • sec • °C | 0.05 | 0.06 | 0.15 | 0.31 | 0.009 | 0.06 | 0.06 | 0.08 | 0.09 | 0.22 | 0.41 |
| | | W/m • K | 21 | 25 | 63 | 130 | 4 | 25 | 25 | 33 | 37 | 91 | 170 |
| **Specific Heat R.T.** | | cal/g • °C | 0.16 | 0.16 | 0.15 | 0.16 | 0.12 | 0.19 | 0.19 | 0.19 | 0.19 | 0.18 | 0.18 |
| **Heat Shock Resistance ΔT** | | °C | 550 | 670 | 400 | 300 | 300 | 300 | — | — | — | 290 | 350 |
| **Volume Resistivity R.T.** | | Ω • cm | $>10^{14}$ | $>^{14}$ | $8x10^{14}$ | $10^3$ | $2x10^{12}$ | $>10^{14}$ | $>10^{14}$ | $>10^{14}$ | $>10^{14}$ | $>10^{14}$ | $>10^{14}$ |

### 2.1.3 Applications of Advanced Ceramics

Ceramics applications could be categorized as structural ceramics, electrical ceramics, ceramic composites, and ceramic coatings. Current and future advanced ceramic products tabulated in Table 2.3. Today, advanced ceramics have been widely used in wearing parts, seals, low weight components and fuel cells in transportation industry, to reduce the weight of product, increase performance especially at high temperatures, prolong the life cycle of a product and improve the efficiency of combustion [17]. To provide some insight into the spectrum of special characteristics and sophisticated applications of advanced ceramics, three important types – structural ceramics, electronic ceramics, and optical ceramics – will be discussed in some details.

**Table 2.3** Current and future products for advanced ceramics [14].

| **Mechanical Engineering** | **Aerospace** | **Automotive** | **Defense industry** |
|---|---|---|---|
| Cutting tools and dies | Fuel systems and valves | Heat engines | Tank power trains |
| Abrasives | Power units | Catalytic converters | Submarine shaft seals |
| Precise instrument parts | Low weight components | Drivetrain components | Improved armors |
| Molten metal filter | Fuel cells | Turbines | Propulsion systems |
| Turbine engine components | Thermal protection systems | Fixed boundary recuperators | Ground support vehicles |
| Low weight components for rotary equipment | Turbine engine components | Fuel injection components | Military weapon systems |
| Wearing parts | Combustors | Turbocharger rotors | Military aircraft (airframe and engine) |
| Bearings | Bearings | Low heat rejection diesels | Wear-resistant precision bearings |
| Seals | Seals | Waterpump seals | |
| Solid lubricants | Structures | | |
| **Biological, Chemical processing engineering** | **Electrical, Magnetic Engineering** | **Nuclear industry** | |
| Artificial teeth, bones and joints | Memory element | Nuclear fuel | |
| Catalysts and igniters | Resistance heating element | Nuclear fuel cladding | |
| Heart valves | Varistor sensor | Control materials | |
| Heat exchanger | Integrated circuit substrate | Moderating materials | |
| Reformers Recuperators | Multilayer capacitors Advanced multilayer integrated packages | Reactor mining | |
| Refractories | | | |
| Nozzles | | | |
| **Oil industry** | **Electric power generation** | **Optical Engineering** | **Thermal Engineering** |
| Bearings | Bearings | Laser diode | Electrode materials |
| Flow control valves | Ceramic gas turbines | Optical communication cable | Heat sink for electronic parts |
| Pumps | High temperature components | Heat resistant translucent porcelain | High-temperature industrial furnace lining |
| Refinery heater | Fuel cells (solid oxide) | Light emitting diode | |
| Blast sleeves | Filters | | |

# CHAPTER 3

# CERAMIC PROCESSING TECHNIQUES

## 3.1 Conventional Ceramic Processing Techniques

Similar to other engineering materials, ceramics have also some limitations in applications, due to their high brittleness and poor workability. There have been intensive research efforts in this field and great progress has been achieved over the past three decades. A scheme for the several types of ceramic-forming techniques is presented in Figure 3.1

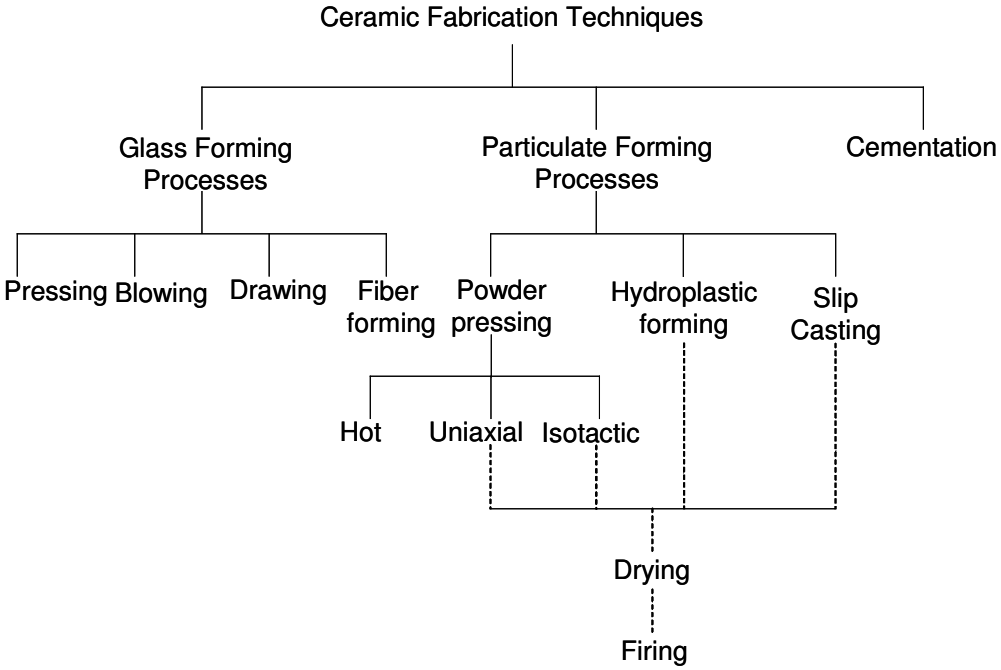


**Figure 3.1** A classification scheme for the ceramic-forming techniques [12].

Many of the metal forming operations rely on casting and/or techniques that involve some form of plastic deformation. Since ceramic materials have relatively high melting temperatures, casting them is normally impractical. Furthermore, in most instances the brittleness of these materials precludes deformation. Some ceramic pieces formed from powders (or particulate collection) must ultimately be dried and fired. Glass shapes are formed at elevated temperatures from a fluid mass that hardens and assumes a permanent set by virtue of chemical reactions. Cements are shaped by placing

into forms a fluid that hardens and assumes a permanent set by virtue of chemical reactions.

### 3.1.1 Glass Forming Processes

Glass is produced by heating the raw materials to an elevated temperature above which melting occurs. Most commercial glasses are of the silica-soda-lime variety. Four different forming methods are used to fabricate glass products: pressing, blowing, drawing, and fiber forming [18]. Pressing is used in the fabrication of relatively thick-walled pieces such as plates and dishes (Figure 3.2). The glass piece is formed by pressure application in a graphite-coated cast iron mold having the desired shape; the mold is ordinarily heated to ensure an even surface. Blowing is completely automated for the production of glass jars, bottles, and light bulbs [12]. From a raw gob of glass, a *parison*, or temporary shape, is formed by mechanical pressing in a mold. This piece is inserted into a finishing or blow mold and forced to conform to the mold contours by the pressure created from a blast of air. Drawing is used to form long glass pieces such as sheet, rod, tubing, and fibers, which have constant cross section [18].

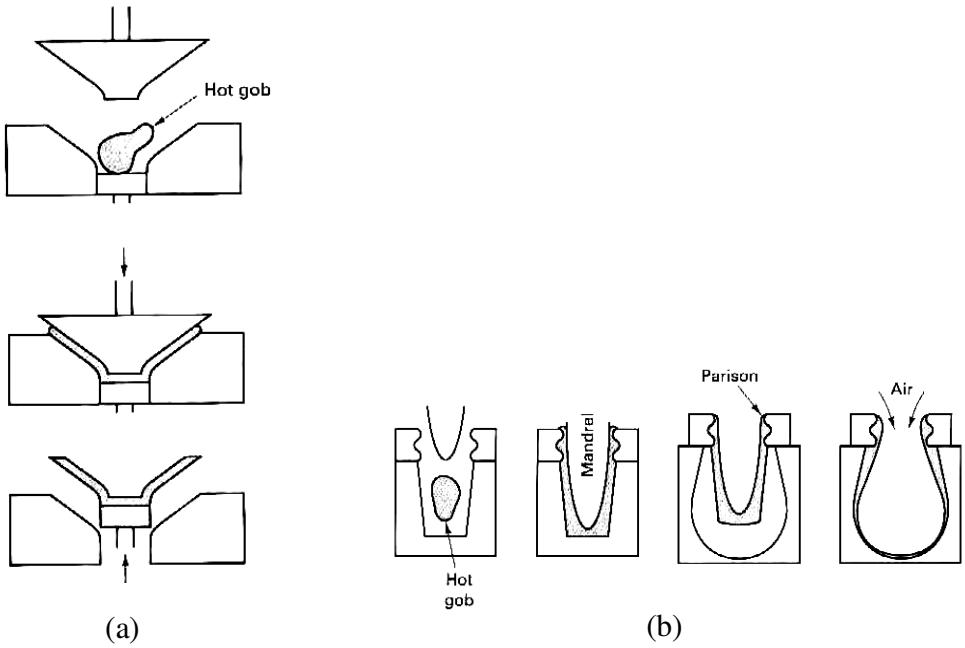


**Figure 3.2** Glass forming by (a) Pressing, (b) Blowing [47].

### 3.1.2 Cementation

Several familiar ceramic materials are classified as inorganic cements: cement, plaster of paris, and lime, which, as a group, are produced in extremely large quantities. The characteristic feature of these materials is that when mixed with water, they form a paste that subsequently sets and hardens [12]. Portland cement is consumed in largest tonnages. It is produced by grinding and intimately mixing clay and lime-bearing minerals in the proper proportions, and then heating the mixture to about 1400$^{o}$C in a rotary kiln: this process is sometimes called **calcinations,** produces physical and chemical changes in the raw material. The resulting "clinker" product is then ground into a very fine powder to which is added a small amount of gypsum ($CaSO_4$-$2H_2O$) to retard the setting process. This product is Portland cement, including setting time and final strength; to a large degree depend on its composition [46].

### 3.1.3 Particulate Forming Processes

#### 3.1.3.1 Powder Pressing (Dry Pressing)

Ceramic ware can be formed under high pressure from powders with relatively low moisture content or often with no moisture at all. The degree of compaction is maximized and fraction of void space is minimized by using coarse and fine particles mixed in appropriate proportions [18]. There are three basic powder pressing procedure. The forming technique, in which powder is compacted in a metal die by pressure applied in one direction, is called uniaxial pressing (Figure 3.3a). It is an inexpensive process with high production rates; however, only simple shapes are possible. In isotactic pressing powdered material is contained in a rubber envelope and the pressure is applied in all directions with same magnitude (Figure 3.3b). More complicated shapes are possible than with uniaxial pressing; however, it is more time consuming and expansive. Both uniaxial and isotactic pressing finishes with drying and firing operations [46]. With hot pressing, the powder pressing and heat treatment are performed simultaneously. This is an expensive fabrication technique that has some limitations. It is costly in terms of time, since both mold and die must be heated and cooled during each cycle. In addition, the mold is usually expensive to fabricate and ordinarily has a short lifetime [13].

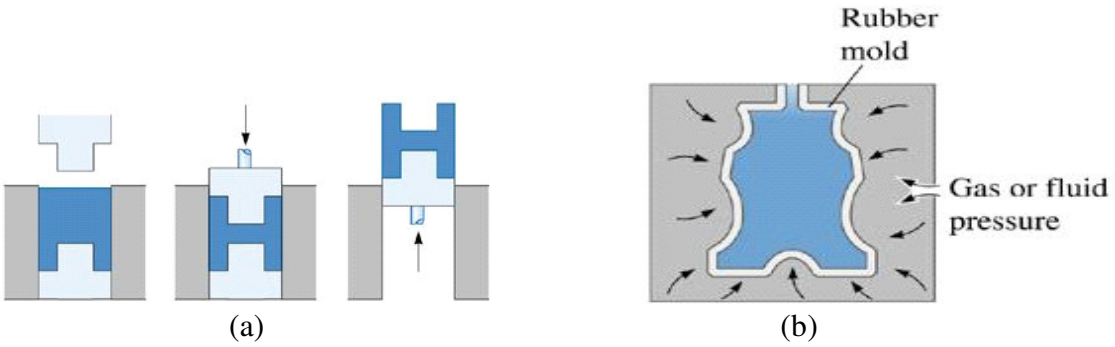


**Figure 3.3** Powder Pressing by (a) Uniaxially, (b) Isotacticly [47].

### 3.1.3.2 Hydroplastic Forming

Clay minerals, when mixed with water, become highly plastic and pliable and may be molded without cracking; however, they have extremely low yield strengths. The water-clay ratio of the hydroplastic mass must give yield strength sufficient to permit a formed ware to maintain its shape during handling and drying. Extrusion is the most common hydroplastic forming technique. A stiff plastic ceramic mass is forced through a die orifice. Constant cross-section is a must. Brick, pipe, ceramic blocks, and tiles are all commonly fabricated by this method [18].

### 3.1.3.3 Slip Casting

A slip is a suspension of clay and/or other nonplastic materials in water. When pored into a porous mold (commonly made of plaster of paris), water from the slip is absorbed into the mold, leaving behind a solid layer on the mold wall that the thickness of which depends on the time (Figure 3.4). This process may be continued until the entire mold cavity becomes solid, or it may be terminated when the solid shell wall reaches the desired thickness, by inverting the mold and pouring out the excess slip. In slip casting, production rates and dimensional precision are low. Slip must have high specific gravity, be very fluid and porable, cast must be free of bubbles. Products have low drying shrinkage and high strength [13].

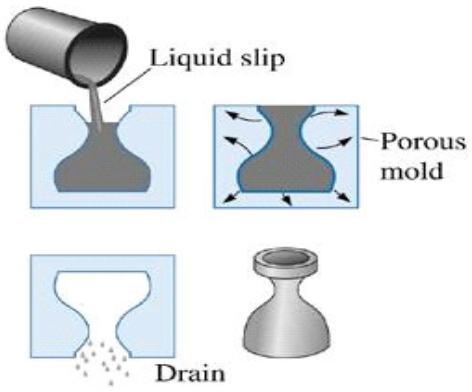


**Figure 3.4** Slip Casting Process [47].

### 3.2 Novel Ceramic Processing Techniques

Advanced ceramics have well-known disadvantages. It is difficult to fabricate them reproducibly because they are brittle, sensitive to microcracking and difficult to machine. Properties of the products are dependent on the purity and physical characteristics of raw materials. Small changes in processing parameters significantly affect their final properties. Traditional advanced ceramic processing techniques require high temperature that is why they are high cost processes and it is hard to produce complex and near-net-shapes. Novel processing techniques which operates at the lower processing temperatures and have potential to easy controlling of improved properties of final products with complex shapes has been essential to be developed. Sol-Gel and polymer pyrolysis techniques are the most recent techniques. Formation of ceramic materials from Si containing polymers has gained a considerable attention due to their unique combination of high purity precursor materials, applicability of versatile plastic shaping technologies and low manufacturing temperatures. Silicon oxycarbide glasses that contain silicon atoms bonded to oxygen and carbon randomly are a group of materials that can be produced by pyrolysis of sol-gel derived precursors or from polymer resins. The replacement of part of the divalent oxygen atom of silica by tetravalent carbon atom leads to an improvement in thermomechanical properties.

### 3.2.1 Sol-Gel Process

The sol-gel process allows synthesizing ceramic materials of high purity and homogeneity by utilization of techniques different from the traditional process of fusion of oxides. This process occurs in liquid solution of organometallic precursors (TMOS, TEOS, Zr(IV)-Propoxide, Ti(IV)-Butoxide, etc.) by means of hydrolysis and condensation reactions (described in Equation 3.1), lead to the formation of a new phase (SOL).

$$\text{M-O-R} + H_2O \rightarrow \text{M-OH} + \text{R-OH (hydrolysis)}$$

$$\text{M-OH} + \text{HO-M} \rightarrow \text{M-O-M} + H_2O \text{ (water condensation)}$$

$$\text{M-O-R} + \text{HO-M} \rightarrow \text{M-O-M} + \text{R-OH (alcohol condensation)} \quad (3.1)$$

(M = Si, Zr, Ti)

The SOL is made of solid particles of a diameter of few hundred of nm suspended in a liquid phase. Then the particles condense in a new phase (GEL) in which a solid macromolecule is immersed in a liquid phase (solvent). Drying the GEL by means of low temperature treatments (25-100 C), it is possible to obtain porous solid matrices (XEROGELs). Heat treatment at temperatures higher than 600$^{o}$C forms dense ceramic structures from xerogels (Figure 3.5) [45].

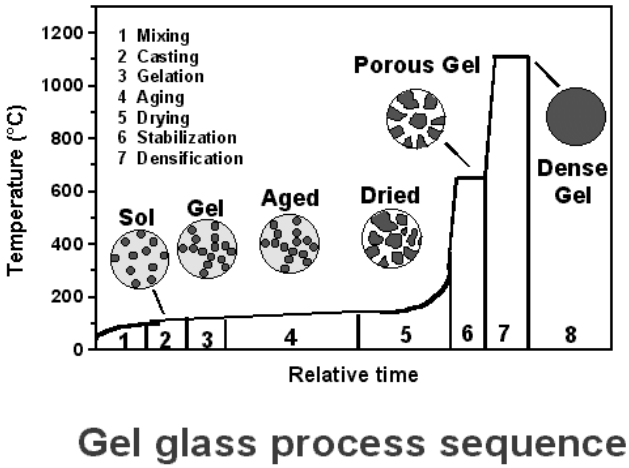


**Figure 3.5** Formation steps of sol-gel glass [45].

The fundamental property of the sol-gel process is that it is possible to generate ceramic material at a temperature close to room temperature. Therefore, such a procedure opened the possibility of incorporating soft dopants, such as fluorescent dye molecules and organic cromophores in these glasses [19]. Thin films can be produced

on a piece of substrate by spin-coating or dip-coating. When the "sol" is cast into a mold, a wet "gel" will form. With further drying and heat-treatment, the "gel" is converted into dense ceramic or glass articles. If the liquid in a wet "gel" is removed under a supercritical condition, a highly porous and extremely low density material called "aerogel" is obtained. As the viscosity of a "sol" is adjusted into a proper viscosity range, ceramic fibers can be drawn from the "sol". Ultra-fine and uniform ceramic powders are formed by precipitation, spray pyrolysis, or emulsion techniques (Figure 3.6) [45].

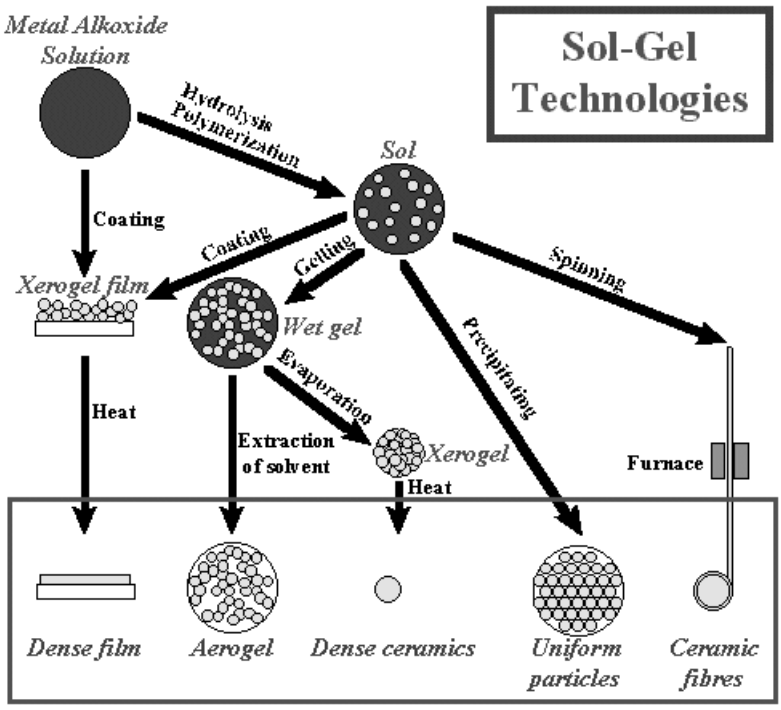


**Figure 3.6** Sol-Gel Technologies and Their Products [45].

### 3.2.2 Polymer Pyrolysis Process

Pyrolysis of polymeric precursor is another way of formation of ceramic structures at low temperatures. Si-containing polymers [$R_{1....2}$,Si(C,N,B,O)$_{0.5.....1.5}$] where R is an organic functional group (for example alkyl, aryl, etc. group) are used for these processes. Cross-linked poly(silanes), -(carbosilanes), -(silazanes), -(siloxanes) and their molecular mixtures are mostly used precursors with high ceramic yields (more than 50 wt% of the initial polymer weight are retained in the ceramic residue) [5]. Polymer pyrolysis technique offers several advantages over conventional melt

processing, as the control of the shape and purity of the final ceramic. In addition, the relatively low temperatures required in these processes allow the preparation of metastable phases. For example, silicon oxycarbide and oxynitride glasses are amorphous materials, characterized by a mixed environment of the silicon atoms, which may be bonded simultaneously to oxygen and carbon in oxycarbide glasses or to oxygen and nitrogen in oxynitride glasses. The replacement of part of divalent oxygen atom of silica by tetravalent carbon atoms or trivalent nitrogen atoms leads to an improvement in the thermomechanical properties. However, because of high temperature degradation reactions and the metastability of these glasses, conventional melt processing is not appropriate for their preparation. On the other hand, the pyrolysis under argon or ammonia of polysiloxane precursors offers a convenient route to respectively silicon oxycarbide and oxynitride glasses (Figure 3.7) [2, 3, 20].

Polymer pyrolysis process can be used in manufacturing a variety of materials as novel binders for ceramic powders, Stuart and co-workers studied on polysilazanes for synthesizing $Si_3N_4$ as binder. The use of traditional, fugitive binders allows for void formation during binder burn off, while the use of binders with high ceramic yields may allow the more facile attainment of high density in the ceramic [23].

For matrix formation in fiber reinforced ceramic composites, ceramic matrix composites are expected to play an important a role in high temperature applications as polymeric matrix composites do at low to medium temperature. The development of cost effective processing techniques remains the key challenge. Processing routes such as slurry infiltration, melt infiltration, chemical vapor infiltration, gas melting reaction, sol-gel and polymer pyrolysis are available for the fabrication of long fiber CMCs. Polymer pyrolysis has been successfully used for fabrication of advanced fibers, such as carbon fiber, silicon carbide fiber and Si-C-N fiber. This technique is also suitable for producing matrices for CMCs, and is particularly attractive as it involves a pressureless pyrolysis process without high pressure sintering. Polysilazanes with backbone Si-N is a desirable candidate for fabrication of $Si_3N_4$ ceramic matrix composites. The chemistry and pyrolytic characteristics of polysilazanes with proper molecular structure and good control of processing parameters can successfully lead to the fabrication of $Si_3N_4$ based composites [24, 25].

For production of coatings, Kawamura et. al. [21] used silicon carbide coatings on a thin high purity of alumina film which was produced from aluminum alkoxide. This alumina film was treated with a polycarbosilane solution and heat treated at

1200°C. The bending strength of the coated alumina film was improved and no electrical resistivity change was observed in the thickness direction [21]. Goerke and co-workers used Si-based inorganic polymers because of their good dissolving properties in an organic solution and exhibiting a sufficiently low viscosity to be processed by spraying. Polymer spraying process has been developed to generate ceramic coatings on different materials by spraying a precursor solution and subsequent pyrolysis. The use of polymer solutions was more successful as compared to polymer melting because of too fast polymerization [22].

Production of ceramic foams was studied by Colombo and co-workers. Porous silicon oxycarbide (SiOC) ceramics in particular bulk and cellular structures were produced via polymer pyrolysis. By using optimal pyrolysis parameters (i.e., heating rate, maximum temperature), the addition of either solid fillers or chemically active additives is efficient in preventing the collapse of pore structure and controlling pore formation through a loss of specific surface area at temperatures above 600°C, whereas slow pyrolysis is able to preserve mesopores up to 1200°C combined with high surface areas. They also investigated the mechanical properties of the ceramic foams obtained through a novel process that uses the direct foaming and pyrolysis of preceramic polymer/polyurethane solutions. The elastic modulus, flexural strength, and compressive strength were obtained for foams in the as-pyrolyzed condition; values up to 7.1 GPa, 13 MPa, and 11 MPa, respectively, were obtained. The strength of the foam was virtually unchanged at temperatures up to 1200°C in air; however, long-term exposure at 1200°C led to a moderate degradation in strength, which was attributed to the evolution of intrastrut porosity during the oxidation of residual free carbon, as well as devitrification of the foam struts. The electric properties of the foams was another scope of Colombo and his co-workers'. The electric properties of the foams were varied by adding suitable fillers to the precursor mixture in amounts up to 80 wt%. The electrical conductivity of the foams was varied by several orders of magnitude. The effect of the type of the filler and preceramic polymer (methylsiloxane or methylphenylsiloxane resins), as well as the used filler precursor, on the properties of the ceramic foams were investigated. While SiC, C, and $MoSi_2$ fillers increased the electrical conductivity even at high filler loadings (9-30 wt%) the presence of copper species led to a dramatic increase of the electrical conductivity even at very small filler loadings (~1 wt%). The presence of copper species seems to affect the carbon structure, which then would play a role in the conduction mechanism [26-28].

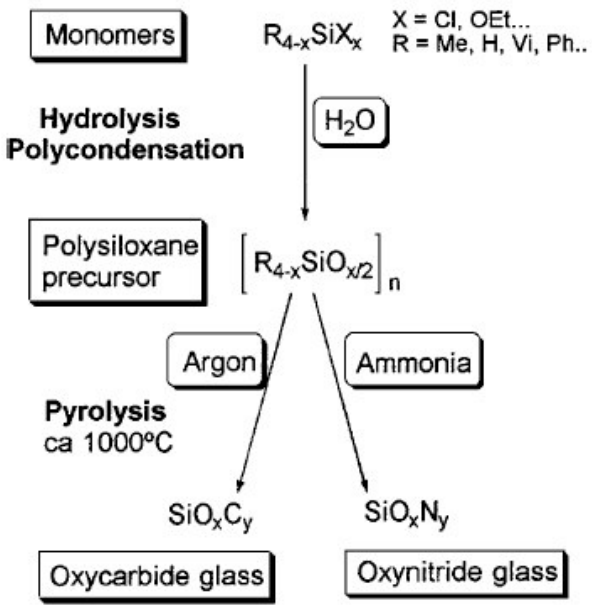


**Figure 3.7** Synthesis of silicon oxycarbide and oxynitride glasses from polysiloxane precursors [2].

### 3.2.2.1 Preceramic Polymers

Inorganic Si-based polymers (silanes, siloxanes, silazanes, carbosilanes, etc.) have been the most commonly studied materials in research. These precursors have polymer constitution in which the desired covalent bonds are already persisting in the as synthesized state and remain in the system through the whole process. The polymer processing has the advantage to avoid any type of powder and their associated problems like agglomerates, particle packing, heterogeneities and high-sintering temperatures. Basically Si-polymers are thermoset materials which start with a comparably short chain precursor and than undergo a network formation either due to heating, radiation, or catalysis. The material is then no longer meltable or soluble but it is still a polymer. Pyrolysis changes the entire molecular structure due to a loss of side groups which leaves an amorphous inorganic glassy material behind [22]. The composition and structure of the glasses depend on the composition and the structure of the precursors and on the reactions that take place during the pyrolysis step. Polymers used in different research and their products are given in Table 3.1.

**Table 3.1** Ceramic products manufactured from basic polymeric precursors.

| Polymer Precursors | | Ceramic Products | References |
|---|---|---|---|
| **Polycarbosilane** | $[ -R_2SiCH_2 -]_n$ | SiC(O) | [29-31] |
| **Polysilazane** | $[ -RSiNH_{1.5} -]_n$ | $Si_3N_4$(C) | [32-35] |
| **Polysiloxane** | $[ -RSiO_{1.5} -]_n$ | $SiO_2$, SiC, C | 2,5,20,36-39 |
| **Polyborosilazane** | $[ -N(BR)_2SiR_2 -]_n$ | $SiBN_xC$ | 40, 41 |

Polysiloxanes have received particular attention as polymeric precursors of silicon oxycarbide glasses ($SiC_xO_y$), because this class of polymers provides an easy and inexpensive route to the formation of such materials [20]. The design of a good precursor (that is a precursor leading in high yields to glass with the desired composition) requires an extensive knowledge of the pyrolysis chemistry of polysiloxanes. Table 3.2 shows some of the precursors pyrolysis products and yields [48].

**Table 3.2** Pyrolysis products and yields [48].

| | Max. Yield (wt%) | | |
|---|---|---|---|
| **Precursor** | **Products** | **Calcd.** | **Obsd.** |
| Carborane-Siloxane (Dexsil, 202) | $SiC/B_4C$ | 64.5 | 60 |
| Carborane-Siloxane (Ucarsil) | $SiC/B_4C$ | 64.5 | 70 |
| 1,1,1,2,3,3,3-Heptamethyl-2-vinyltrisilane | SiC | 60 | 50 |
| Polyfurfuryl alcohol ester | Glassy Carbon | 60 | 50 |
| Poly(borodiphenyl)siloxane | $SiC/B_4C$ | 43 | 43 |
| Ammonioborane | BN | 81 | 65 |
| Boronylpyridine | $B_4C$ | 27 | 22 |
| Alkalenetrisilazane | $SiC/Si_3N_4$ | 20 | 10 |
| Tetraphenylsilane | SiC | 50 | 6 |
| N,N-Diphenyltetraphenylcyclodisilazane | $SiC/Si_3N_4$ | 15 | 5 |
| Diphenyldipropenylsilane | SiC | 15 | 3 |
| Triphenylvinylsilane | SiC | 69 | 2 |
| Carborane | $B_4C$ | 78 | 2 |
| Phenyltrimethylsilane | SiC | 27 | 1 |
| Triphenylsilane | SiC | 15 | 1 |
| N-6,9-Bis(trimethylsily)adenine | $SiC/Si_3N_4$ | 33 | 1 |
| Triphenylboron | $B_4C$ | 23 | <1 |
| Trimethylaminoborine | $BN/B_4C$ | - | 0 |
| Bis(diethylamino)dimethylilane | $Si_3N_4/SiC$ | - | 0 |
| Polydimethylsilane | SiC | - | 0 |
| 1,1,3,3-Tetramethyldisilazane | $Si_3N_4/SiC$ | - | 0 |
| Tetramethylammonium tetrahydroborate | $BN/B_4C$ | - | 0 |

### 3.2.2.2 Pyrolysis Chemistry of Polysiloxane Precursors

The pyrolysis of linear polysiloxanes usually leads to zero or poor ceramic yields. This may be ascribed to the occurrence of *depolymerization* reactions (Figure 3.8), involving the redistribution of Si-OSi/Si-OSi bonds or the nucleophilic attack of silanols, which lead to the formation of volatile cyclic oligomers. Conversely, highly cross-linked polysiloxanes lead to much higher ceramic yields. In this case, the depolymerization reactions are hindered by the lack of mobility of the chains (Figure 3.9). Moreover, several depolymerization steps are required to fragment the polymer network, and the fragments formed are of low volatility.

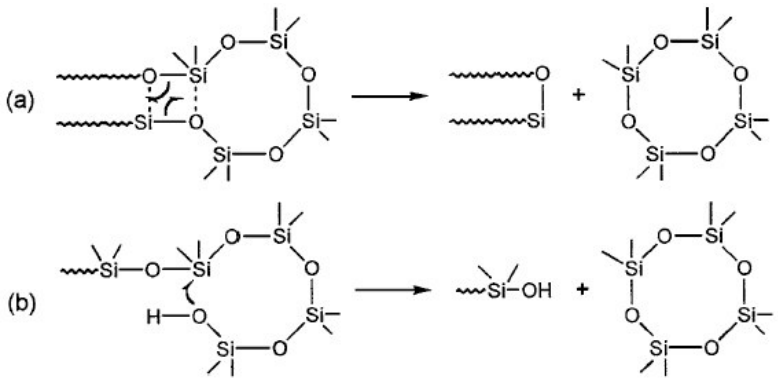


**Figure 3.8** Depolymerization reactions in linear polysiloxanes by (a) redistribution of Si-OSi/Si- OSi bonds or (b) nucleophilic attack of terminal silanols [2].

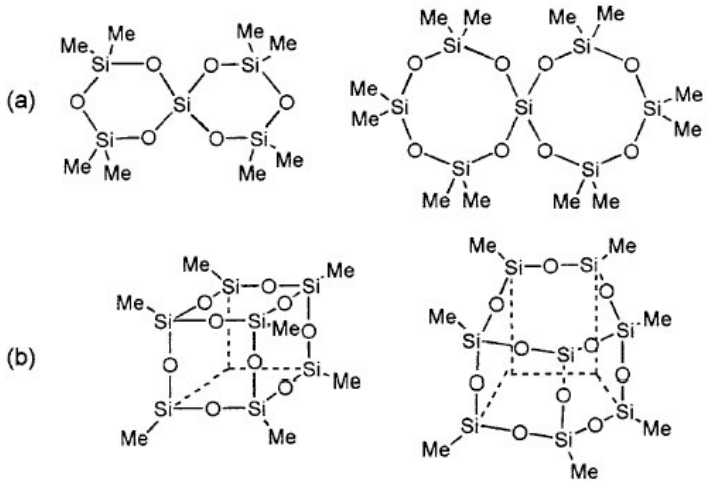


**Figure 3.9** Examples of thermal depolymerization products of cross-linked polysiloxanes containing (a) $Me_2SiO$ (D) and $SiO_2$ (Q) units or (b) $MeSiO_{1.5}$ (T) units [2].

Most of the polysiloxane gel precursors contain residual silanol groups, which certainly play an important part in the depolymerization, as in linear polysiloxanes, unless they are consumed before this step. Apart from Si-OH/Si-OH *condensation*, leading to the formation of siloxane linkages and water (Figure 3.10(a)), these silanols may be consumed by condensation with Si-R groups (Figure 3.10(b)). The cleavage of Si-H bonds by this reaction takes place above 250°C, the cleavage of Si-Ph bonds above ca. 300°C, as in linear PMPS. On the other hand, the cleavage of aliphatic Si-C bonds by Si-OH apparently requires a much higher temperature, above 500°C.

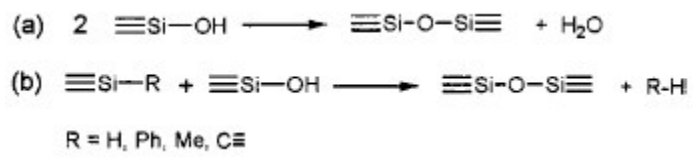


**Figure 3.10** Condensation reactions involving silanols [2].

The increased thermal stability of cross-linked polysiloxanes permits the occurrence of *redistribution* reactions involving the exchange of Si-O bonds with Si-H bonds (above 300°C) or Si-C bonds (above 500°C). These reactions are characterized by the formation of new siloxane units $SiO_xX_{4-x}$ (readily evidenced by $^{29}Si$ NMR), as illustrated in Figure 3.10(a) for a silsesquioxane gel. It is noteworthy that heating at 500°C a gel built of D and Q units leads to the formation of T units, which illustrates the reversibility of such reactions. Successive redistribution steps may lead to the formation of volatile silicon compounds, such as $SiH_4$ in the case of $HSiO_{1.5}$ gels, or $Me_3SiOSiMe_3$ in $MeSiO_{1.5}$ gels (Figure 3.10(b) and (c)).

At high temperature (between 500 and ca. 1000°C), reactions involving the cleavage of Si-C, C-C and C-H bonds occur, leading to the escape of hydrocarbons and hydrogen and to the formation of an inorganic material. The formation of the gases may be accounted for by simple mechanisms, involving the formation of free-radicals by homolytic bond-cleavage, followed by hydrogen abstraction, combination or rearrangement (Figure 3.12(a)).

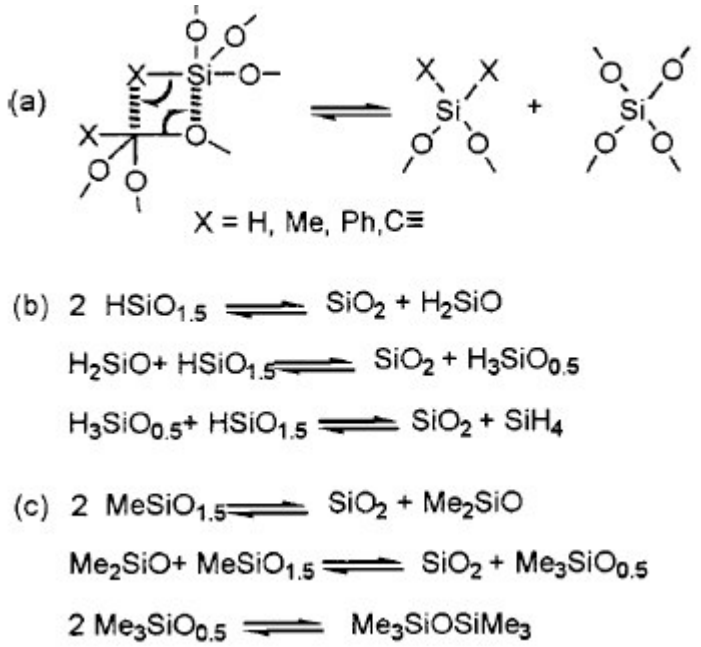


**Figure 3.11** Redistributions involving the exchange of Si-C or Si-H bonds with Si-O-Si bonds: (a) Schematic representation (silsesquioxane units); (b) Formation of $SiH_4$ by successive Si-H/Si-O redistribution steps from a $HSiO_{1.5}$ gel; (c) Formation of $Me_3SiOSiMe_3$ by successive Si-Me/Si-O redistribution steps from a $MeSiO_{1.5}$ gel [2].

At high temperature (between 500 and ca. 1000°C), reactions involving the cleavage of Si-C, C-C and C-H bonds occur, leading to the escape of hydrocarbons and hydrogen and to the formation of an inorganic material. The formation of the gases may be accounted for by simple mechanisms, involving the formation of free-radicals by homolytic bond-cleavage, followed by hydrogen abstraction, combination or rearrangement (Figure 3.12(a)). The formation of the residue is much more complex, and only general trends may be given. As long as hydrogen atoms are abundant, the most probable reaction is hydrogen abstraction. As the temperature increases, the hydrogen atoms become less and less abundant, due to the escape of $H_2$ and hydrocarbons, and the rate of bond cleavage increases. The probability of combination between Si and C free-radicals becomes more and more important, producing an increase of the cross-linking around Si and C atoms. Successive bond cleavages, combinations and rearrangements gradually lead to the formation of the $CSi_4$ units of the oxycarbide phase. For instance, in the case of methylated precursors, the intermediate formation of Si-$CH_2$-Si species at 750°C has been evidenced by IR spectroscopy. The formation of such species may be well accounted for by a free-radical mechanism (Figure 3.12(b)).

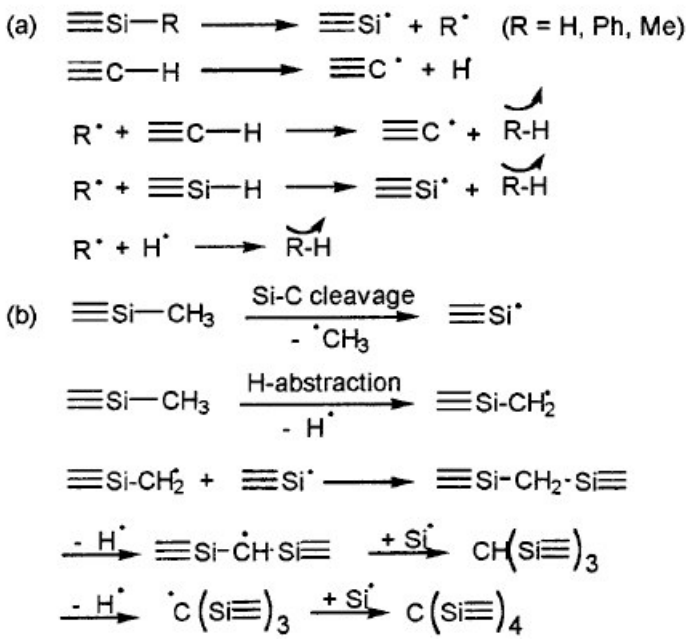


**Figure 3.12** Mineralization step: (a) formation of gases and generation of ≡Si· and ≡C· free radicals; (b) formation of $CSi_4$ tetrahedra (methylated precursor) [2].

Above ca. 1450°C, silica reacts with carbon to give silicon carbide and carbon monoxide. The overall reaction is given in Figure 3.13(a). In a silicon oxycarbide glass, of composition $SiO_xC_y$, the reaction products depend on the amount of carbon in the glass. When the carbon content is high enough (y >1+x), the carbothermal reduction leads to the formation of silicon carbide and free-carbon with an escape of carbon monoxide only (Figure 3.13(b)). This reaction was used to prepare silicon carbide from polysiloxane precursors. When y is lower than 1+x, the carbothermal reduction leads to the formation of SiC with loss of carbon monoxide and silicon monoxide (Figure 3.13(c)).

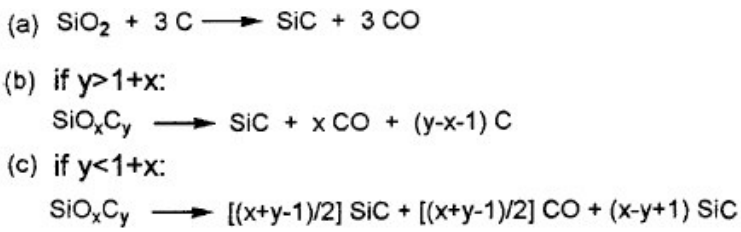


**Figure 3.13** Carbothermal reductions of silica (a) and $SiO_xC_y$ glasses (b, c) [2].

### 3.2.3 Active Filler Controlled Polymer Pyrolysis Process

Polymer pyrolysis is a relatively new and very promising technique for processing of advanced ceramics in the form of powder particles, thin films and/or protective coatings as well as fibers. The major advantages of such polymer-derived materials are their intrinsic homogeneity on the atomic level, the rather low processing temperatures, and the use of established polymer-processing techniques that enable complex shaping. However, the applicability of subsequent polymer pyrolysis to the fabrication of monolithic components is quite difficult, in particular, owing to the high volume shrinkage associated with the polymer-ceramic transition that often leads to the development of intrinsic microcracks.

In general, processing of ceramic monoliths via organometallic compounds involves crosslinking of the starting precursor followed by pyrolysis at elevated temperatures either in inert or reactive atmospheres. The applied heat treatment initiates the organic-inorganic transition and results in the formation of an amorphous covalent ceramic. Annealing at temperatures exceeding 1000$^{o}$C yields a partially or completely crystallized ceramic material, which commonly reveals both a residual porosity up to 15% and in some cases a high microcrack density. To overcome this latter problem, a modified process, active filler controlled pyrolysis (AFCOP), has been developed by Greil and co-workers [5-7]. The concept became a scope of many other researches recently [3, 8-11].

According to this method, the polymer is partially filled with inert or active powder particles in order to decrease the shrinkage and to allow the fabrication of bulk, crack free ceramics. Employing active fillers, a reaction between the filler particles and the precursor is initiated which typically results in a volume expansion of the reaction product, as compared to the starting compounds. This expansion counteracts the shrinkage during densification and can lead to near-net shaped crack-free components. Suitable active fillers are elements or compounds such as Al, B, Si, Ti, $CrSi_2$, $MoSi_2$, etc. forming carbide, nitride, or oxide reaction products which exhibit a high specific volume increase upon reaction. Ceramic fillers like AlN, $B_4C$, etc. offer the possibility of forming matrices of the sialon, mullite or borosilicate type when reacting with the siloxane polymer, for example. When metal oxide fillers such as NiO, $Mn_2O_3$, CuO, etc. are used, reduction of the active filler results in the formation of the novel ceramic composite materials containing highly dispersed metal or metal silicide particles. The

active fillers can be combined or partly replaced by inactive fillers which do not react during the pyrolysis process but can provide specific functionality to the ceramic material. Thus, for adjusting elasticity, thermal expansion, electrical resistance, etc. inactive fillers offer an additional degree of freedom for tailoring the material properties. When utilizing inert fillers, simply the precursor volume is reduced which lowers the volumetric changes of the sample (Figure 3.14).

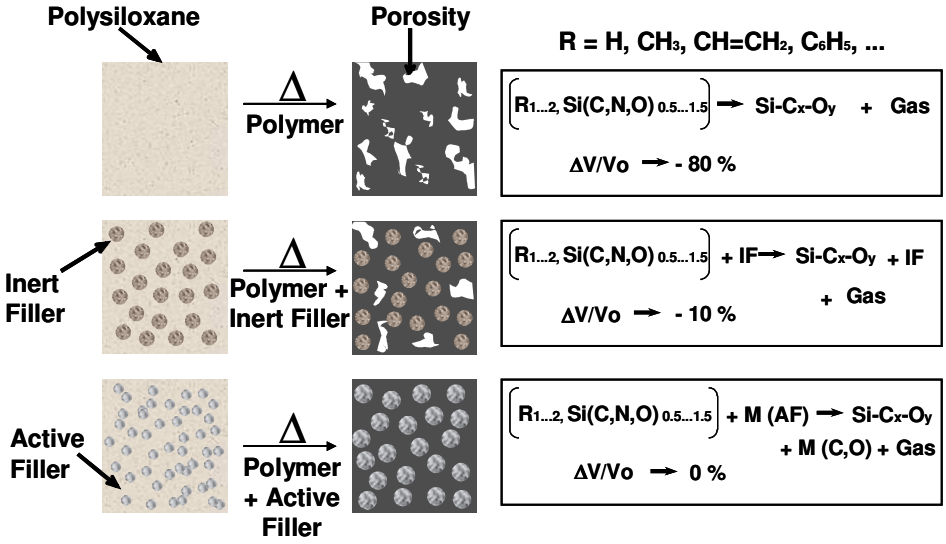


**Figure 3.14** Effect of active/inert filler addition on final ceramic structure [5].

Polymer/filler reactions that can be occurred as a function of increase in pyrolysis temperature may be described as below:

1. In between 600-800°C: an organic-inorganic transformation, leading to an amorphous hydrogenated oxycarbide built on tetrahedral structures of the type Si ($C_aO_b$) with a + b = 4 depending on the initial polymer composition.
2. Above 800°C: Precipitation of excessive carbon to form a network of turbostratic carbon.
3. 1100-1600°C: Nucleation of crystalline precipitations such as SiC and $SiO_2$ (Equation 3.2).
4. Grain coarsening that results in consumption of the residual amorphous phase and reduction of oxygen content due to evaporation of SiO and CO.

$$Si - O_a - C_b\ (am)\ (s) \rightarrow (1\text{-}1/2)\ SiC\ (s) + a/2\ SiO_2\ (s) + (a/2 + b - 1)\ C\ (s) \qquad (3.2)$$

Depending on their reactivity, filler particles begin to react with solid or gaseous decomposition products at 400°C (Ti) or 1300°C (B).

In the presence of reactive filler, solid carbon and gaseous hydrocarbon species can react to form carbide phases resulting in a significant increase of ceramic yield (Equation 3.3).

$$[RSiO_{1.5}](s) + F(s) \rightarrow Si\text{-}O\text{-}C(s) + FC_x(s) + H_2(g) \quad (3.3)$$

For example, poly(phenyl)siloxane loaded with Ti and pyrolyzed in Ar-atmosphere at 1000°C yields a siliconoxycarbide composite (Equation 3.4)

$$[(C_6H_5)SiO_{1.5}](s) + Ti(s) \rightarrow Si\text{-}O\text{-}C(s) + TiC(s) + CH_x(g) + H_2(g) \quad (3.4)$$

where $CH_x$ mainly represents $C_6H_6$. When pyrolysis is carried out in a reaction atmosphere, the filler particles can react with the gaseous phase present in the open pore network, which forms during polymer decomposition between 400 and 800°C (transient porosity) or due to carbothermal decomposition at temperatures above 1000°C. For example, reaction of poly(phenyl)siloxane with $CrSi_2$ in $N_2$-atmosphere at 1400°C yields an oxycarbonitride ceramic composite (Equation 3.5).

$$[(C_6H_5SiO_{1.5}](s) + CrSi_2(s) + N_2(g) \rightarrow Si\text{-}O\text{-}C\text{-}N(s) + Cr_3C_2(s) + Si_3N_4(s) + CH_x(g) \quad (3.5)$$

If the carbon activity at the filler particle surface is sufficiently high ($a_c > 0.1$), carbon generated by polymer decomposition reacts with chromium, whereas silicon reacts with nitrogen from reactive atmosphere to form a carbide/nitride scale of the $Cr_3C_2$-$Si_3N_4$ type on the filler particle surface. The deriving force to form nitrides can be increased with increasing external nitrogen pressure. Reaction of poly(methyl)siloxane with B in $N_2$-atmosphere at 1500°C (Equation 3.6)

$$[(CH_3)SiO_{1.5}](s) + B(s) + N_2(g) \rightarrow Si\text{-}O\text{-}C\text{-}N(s) + BN(s) + Si_2N_2O(s) + CH_x(g) \quad (3.6)$$

results in the formation of nitride and oxynitride reaction products. Due to a specific volume increase of +39% from $CrSi_2$ to ($Cr_3C_2$ + $Si_3N_4$) and even +142% from B to BN zero shrinkage polymer-ceramic transformation can be obtained with volume fraction of 30-40%.

# CHAPTER 4

# EXPERIMENTAL

## 4.1 Materials

Two different preceramic polymers, poly(phenyl)siloxane (PPS) (H62C, Wacker Chemie, GE) and poly(methyl)siloxane (PMS) (MK, Wacker-Belsil, GE) were used. PPS was used as received while PMS was a solid solvent free resin, which was dissolved in toluene and mixed with Zr-acetylacetonate. As inert filler, SiC with particle sizes in the range of 10-40 µm, and active filler, Ti with particle size of -149 µm were used.

## 4.2 Processing of Neat Silicon Oxycarbide Ceramics

To monitor the thermal transformation of the preceramic polymers neat polymers without any filler addition were prepared. Figure 4.1 shows the processing stages to prepare ceramics without filler addition and composite (CMC) samples as well.

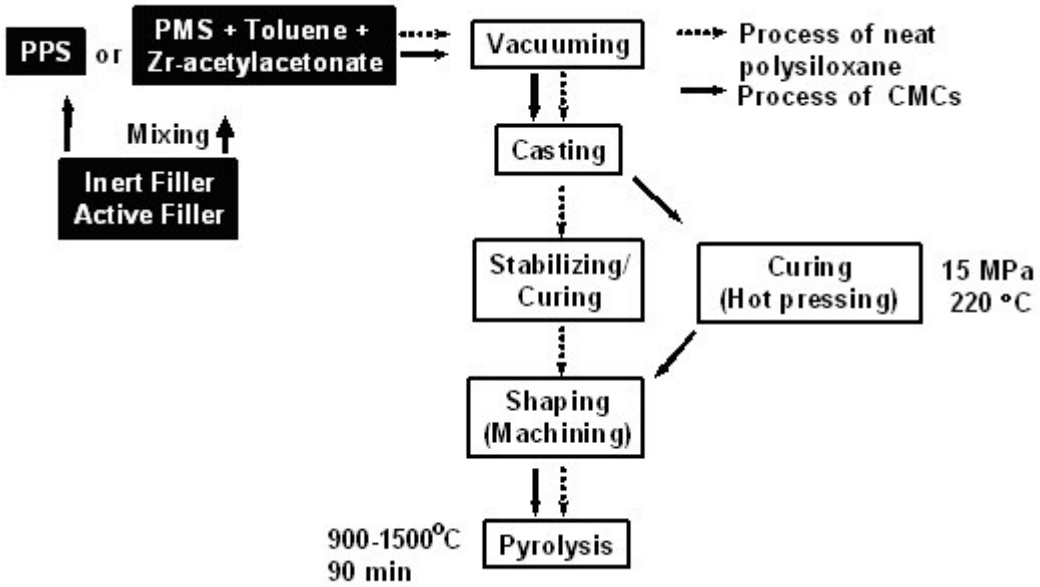


**Figure 4.1** Ceramic composite processing with PPS and PMS preceramic polymers.

Polymers (after addition of catalyst for PMS) were vacuumed for half an hour and casted in Teflon moulds and cured in an oven at 220°C under open-air atmosphere. Parts were machinable with convenient tools (drilling, cutting, milling, etc.). Pyrolysation of the neat samples took place in a tubular furnace operated under inert argon atmosphere at various temperatures (900-1500°C). A typical heating cycle involved heating to 400°C at 5°C/min, held at this temperature for 30 min, then a second ramp to 530°C at 5°C /min, held at this temperature for 60 min and heating to the final temperatures ($T_u$) at 5°C/min and held the sample for 90 min at $T_u$ and finally cooling the samples to the room temperature (Figure 4.2). In addition to inert argon, specimens were prepared under reactive nitrogen atmosphere based on the same preparation treatment.

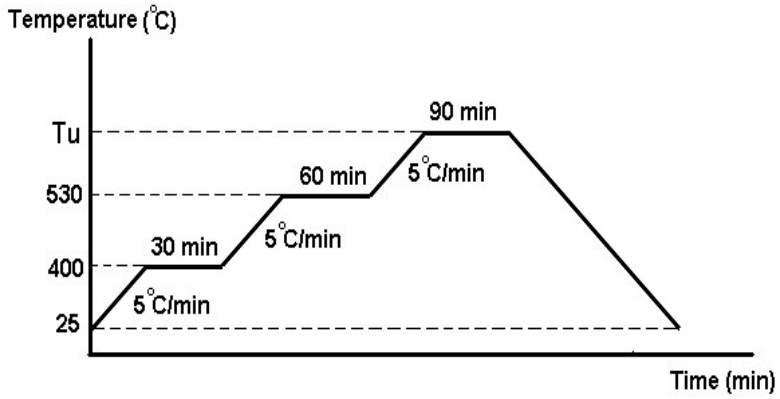


**Figure 4.2** A typical pyrolysis schedule.

### 4.3 Processing of Composite Monoliths

To monitor the effect of filler addition on the microstructural and mechanical properties of the composites, composite samples were prepared (Table 4.1). To prepare ceramic composites, inert and active powders were mixed with the polymers at various ratios in the range of 60-80 wt% to obtain green bodies (Figure 4.1). Blends were casted in metal moulds, partially stabilized in an oven at 150°C and then uniaxially pressed using a hot press under 15 MPa at 220°C for 2 hours for complete curing. After cutting the specimens in the desired dimensions, green bodies were finally pyrolyzed following a multi-step heating schedule shown in Figure 4.2.

**Table 4.1** Composite monoliths prepared within the study.

| Polymer Type | Filler Type | Filler Ratio | Pyrolysis Temperature ($^oC$) | Atmosphere |
|---|---|---|---|---|
| Poly(phenyl)siloxane | Ti | 60, 70, 80 | 900, 1100, 1300, 1500 | Ar, $N_2$ |
| | Si | | | |
| | SiC | | | |
| | $Al_2O_3$ | | | |
| Poly(methyl)siloxane | Ti | | | |
| | Si | | | |
| | SiC | | | |
| | $Al_2O_3$ | | | |

## 4.4 Monitoring of Thermal Conversion of Polysiloxanes and Characterizations of Ceramics

Pyrolytic conversion of the preceramic polymers to ceramic structures was monitored by a variety of analytical techniques. Also, the effect of the filler addition on the microstructure, thermal transformations and mechanical properties of the specimens were investigated or compared to the properties of the neat samples.

### 4.4.1 X-Ray Diffraction Method

Pyrolysis products of neat and composite samples were identified by X-ray diffraction (XRD) technique using Philips X'Pert Pro diffractometer, with CuKα radiation. Samples pyrolysed at elevated temperatures (900-1500$^oC$) were powdered and analyzed at diffraction angles (2θ) between 5-70$^o$. Using XRD, the effect of the temperature and filler type on phase developments were characterized.

### 4.4.2 Scanning Electron Microscopy (SEM)

Microstructure of the neat and composite specimens was characterized using SEM. Polished samples were prepared by first cutting and then molding the samples in molding resin. Grinding and polishing was performed using papers in the size of 180, 240, 400, 600, 800, 1000, and 1200 and diamonds of 9, 6, 3, and 1 μm size. Philips XL 30SFEG field emission scanning electron microscope (SEM) and attached energy dispersive X-ray (EDX) spectrometer was utilized to analyze polished and fractured

specimen surfaces. Back scattered electron images of the composite samples was also used to identify the distribution of filler particles in polymer matrix.

### 4.4.3 Infrared Spectroscopy Technique (FTIR)

Infrared spectroscopy technique (FTIR) was also used to identify the phase changes by pyrolytic heat treatment using Nicolet Magna-IR 550 Spectrometer. Samples after curing at 150$^{o}$C and pyrolyzing at elevated temperatures (900-1500$^{o}$C) were ground and analyzed.

### 4.4.4 Thermal Analysis (TGA-DTA)

Thermal analyses were performed for determination of the mass changes and phase developments with different filler addition. Samples were pyrolyzed at 1300$^{o}$C with 5$^{o}$C/min heating rate under reactive $N_2$ atmosphere.

### 4.4.5 Optic Microscopy

Using optic microscope, particle and pore dispersion in the composite structure were identified. Nikon Eclipse L150 optic microscope was used for the analysis of the polished samples.

### 4.4.6 Determination of Mass Losses and Densities

Effect of the filler type, ratio and pyrolysis temperature on the mass losses and density changes was measured. Mass loss determinations were done based on the weight of samples before pyrolysis ($m_1$) and weight after pyrolysis ($m_2$) from equation (4.1)

$$\%Mass\ Change = \frac{m_1 - m_2}{m_1} \times 100 \tag{4.1}$$

Thermogravimetric analysis was also being carried out for determination of the mass changes. To monitor the effect of filler type and pyrolysis temperature on density

changes Archimedes method was used. Measurements were performed using Precisa XB 220A Archimedes measurement kit.

### 4.4.7 Vickers Indentation Tests

The hardness values of the ceramics without filler addition and composite samples were measured by Vickers indentation test to investigate the effect of filler type, its weight fraction and pyrolysis temperature on the mechanical behavior of the samples. Polished samples were also used for indentation tests with HV10 (100N) using Zwick/Roell-TestX'Pert V9.0 machine. The indentation tip displacement rate was selected as 0.2 mm/min.

# CHAPTER 5

# RESULTS AND DISCUSSION

## 5.1 Thermal Conversion of Polysiloxane

Green bodies were obtained after polymerization of the precursors at 220°C. The stability of green bodies indicated the network formation. The organic to inorganic conversions were studied by IR spectroscopy and X-Ray diffraction techniques. Figure 5.1 shows the XRD patterns of the neat poly(phenyl)siloxane (PPS) samples pyrolyzed at different temperatures. The patterns up to 1300°C are characteristic of amorphous materials of $SiO_xC_y$. The broad peaks with low intensities at above 1300°C are the diffractions associated to β-SiC. The peaks of $2\theta = 36°$ and 60° at 1500°C are characteristic for β-SiC crystals.

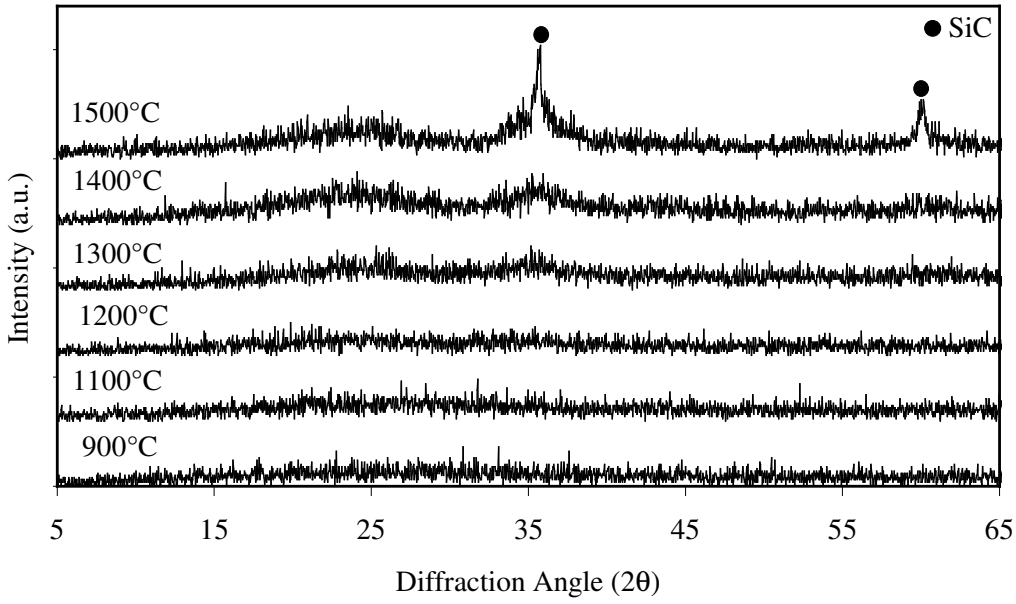


**Figure 5.1** X-ray diffraction patterns of the poly(phenyl)siloxane (PPS) without filler addition pyrolyzed under Ar at various temperatures.

Figure 5.2 shows the XRD patterns of the PMS after pyrolysis at various temperatures. As seen from the patterns the formation of β-SiC crystals occurs with low

intensities at 1500°C at diffraction angles 2θ = 36° and 60°, whereas an amorphous structure can be observed at lower temperatures.

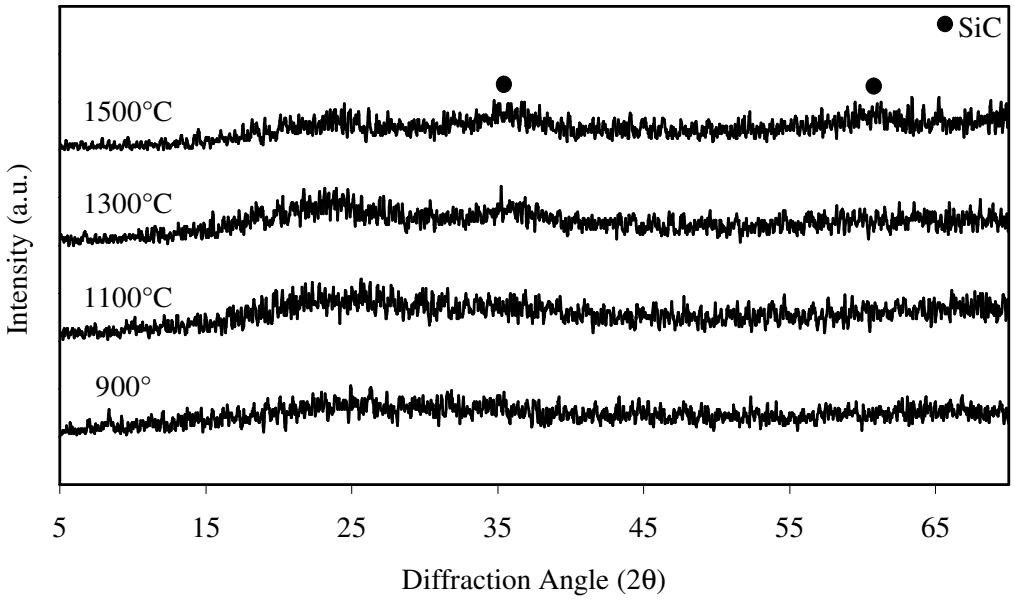


**Figure 5.2** X-ray diffraction patterns of the poly(methyl)siloxane (PMS) without filler addition pyrolyzed under Ar at elevated temperatures.

The thermal conversion from organic siloxane network into the inorganic ceramic structure was also investigated using FTIR method. Figure 5.3 shows the infrared spectra of the PMS polymer without filler addition processed at various temperatures. The spectra give the vibration bands of 770 (assym. n Si-$CH_3$), 1030 (Si-OR), 1120 (Si-O-Si), 1280 (sym. Si-$CH_3$) and a broad band between 2000-3000 (SiOC-H) for the samples prepared at 220°C. After pyrolysation of the samples above 1100°C, the volatile hydrocarbons release from the structure, which is in agreement with the FTIR results, no C-H absorption bands, was detected.

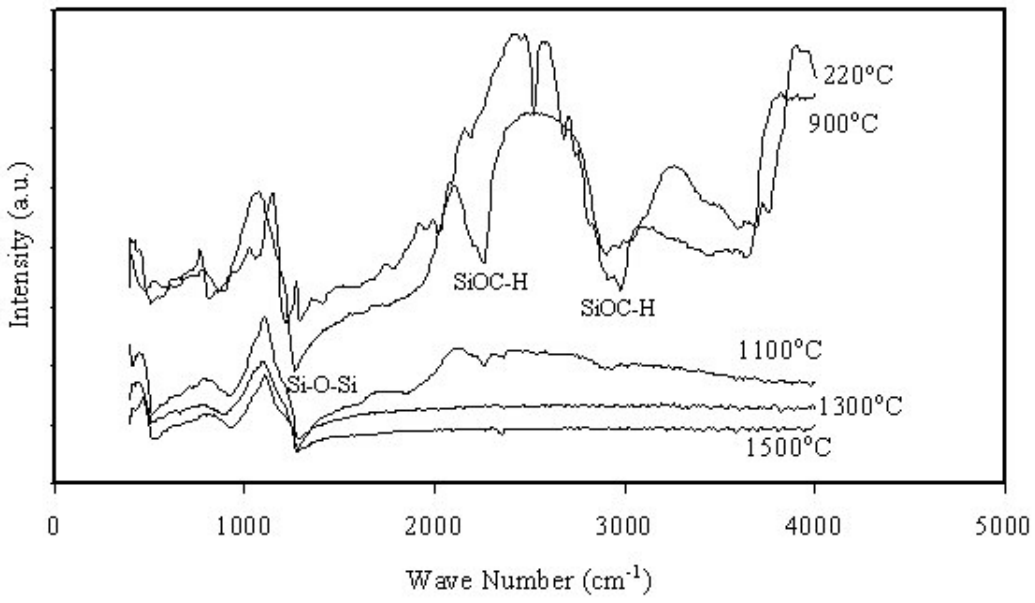


**Figure 5.3** FTIR of the poly(methyl)siloxane (PMS) without filler addition after polymerization at 220°C and pyrolysis under Ar at various temperatures.

Figure 5.4 shows the fracture surface SEM micrographs of the pyrolysis products of the PPS processed at various temperatures. At lower temperatures, glassy surfaces with low porosity were observed. Higher pyrolysis temperatures yielded uniformly distributed submicron sized pores formed due to the density changes from the polymer to the ceramic phases. SEM-EDX analyses were performed on the same surfaces and the chemical composition of the pyrolysis products at various temperatures are listed in Table 5.1. The SEM-EDX analysis for these samples also confirms the formation of the SiOC structure.

The microstructure of the PMS samples without filler addition pyrolyzed at elevated temperatures is different as compared to PPS samples. Pore formations cannot be observed with this polymer (Figure 5.4); however SiOC structure formations was monitored again by EDX analysis (Table 5.1). Different microstructure of these samples may be the result of methyl containing structure of the precursor.

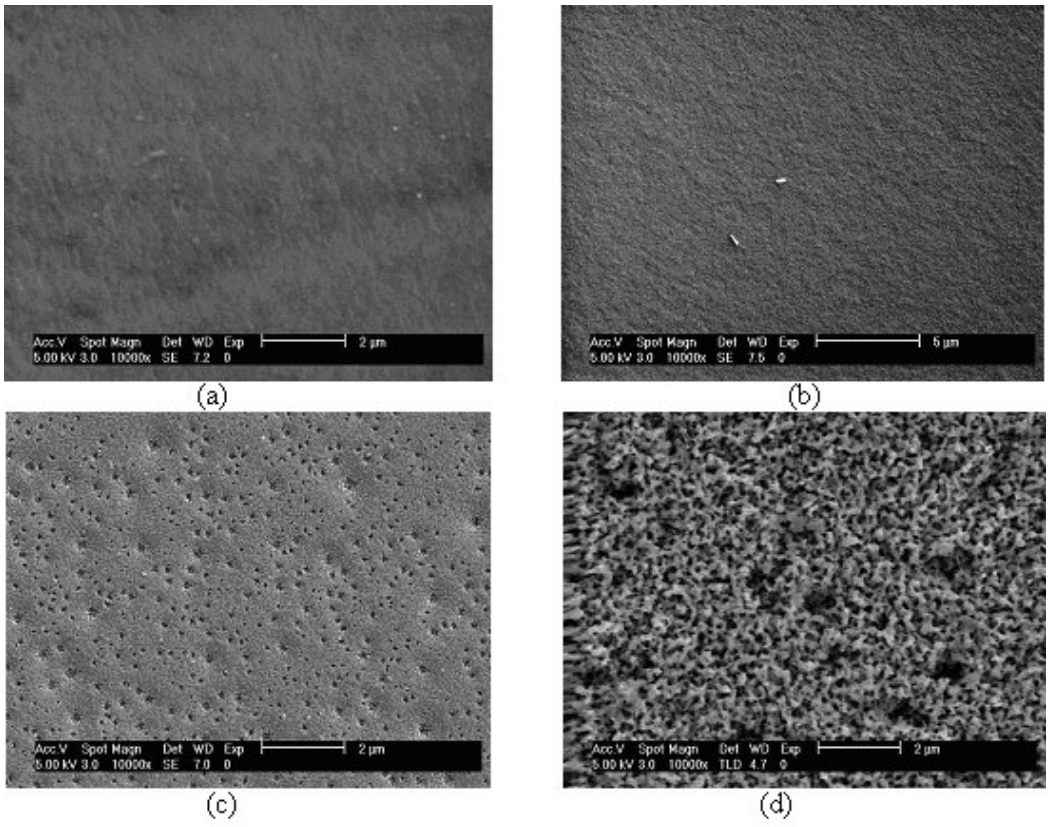


**Figure 5.4** Fracture surface SEM images of PPS samples without filler addition pyrolyzed at (a) 900°C, (b) 1200°C, (c) 1400°C, (d) 1500°C.

**Table 5.1** SEM-EDX analysis of PPS samples without filler addition pyrolyzed at elevated temperatures.

| | | Average wt.% | | |
|---|---|---|---|---|
| **Sample** | **Pyrolysis Temperature(°C)** | **C** | **O** | **Si** |
| **PPS** | 900 | 47 | 20 | 3 |
| | 1200 | 34 | 28 | 39 |
| | 1300 | 9 | 36 | 55 |
| | 1400 | 41 | 15 | 44 |
| **PMS** | 900 | 26 | 54 | 20 |
| | 1100 | 21 | 41 | 39 |
| | 1300 | 15 | 46 | 39 |
| | 1500 | 23 | 38 | 40 |

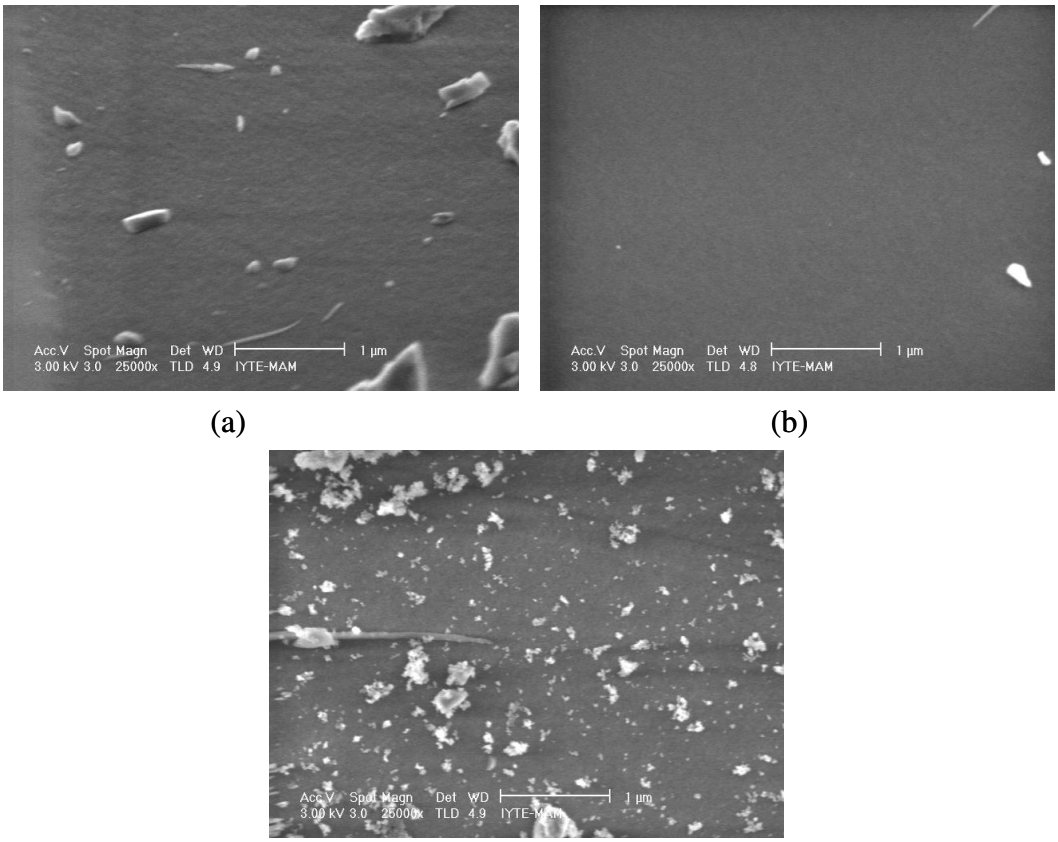


**Figure 5.5** Fracture surface SEM images of PMS samples without filler addition pyrolyzed at (a) 1100°C, (b) 1300°C, (c) 1500°C.

## 5.2 Microstructural Features of Si-O-C Based Ceramic Composites

Monolithic CMC structures with active and inert filler incorporation were prepared at various pyrolysis temperatures. Figure 5.6 is an example showing the SE and BSE images of the green bodies of Ti/PMS sample before pyrolysation. As seen from the figures, a uniform distribution of the particles within the polymer matrix occurs by blending and hot pressing of the materials. Figure 5.7 shows the SEM image of the same Ti/PMS system before and after pyrolysation. As can be observed from the figure, the microstructure of the CMC is changing after pyrolysation of the samples.

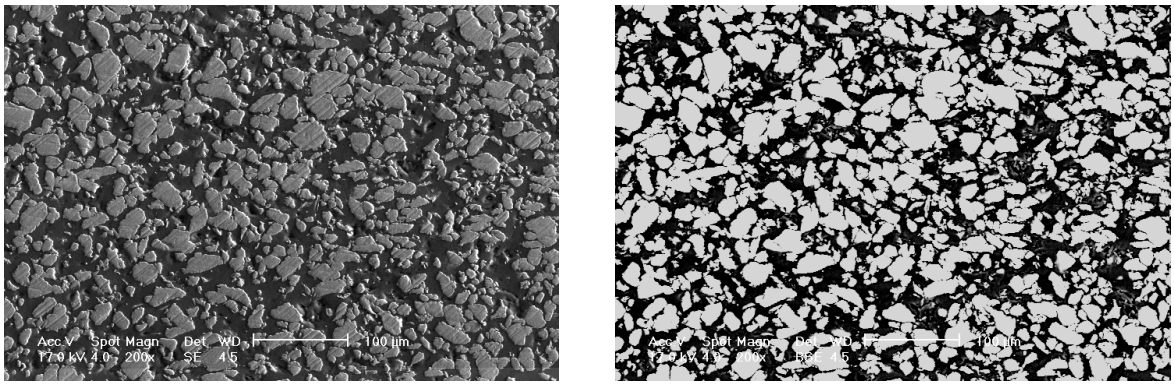


(a) (b)

**Figure 5.6** SEM micrographs of 70 wt% Ti /PMS system before pyrolysis (a) SE image (b) BSE image.

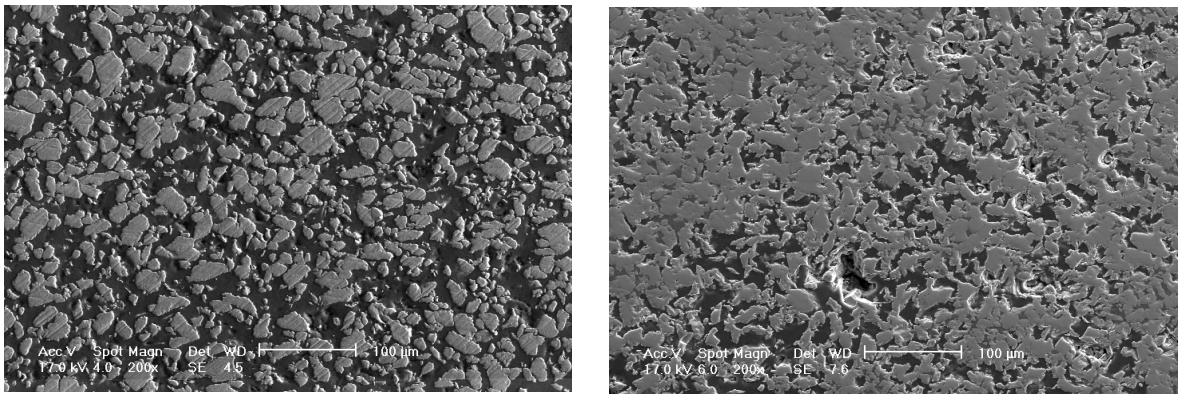


(a) (b)

**Figure 5.7** SEM micrographs of 70 wt% Ti /PMS system (a) before pyrolysis (b) pyrolyzed under Ar at 1100$^{o}$C.

The effect of the filler type and ratio, pyrolysis temperature and atmosphere on the microstructural features of the samples was investigated. Figure 5.8 and 5.9 show the XRD patterns of the 60wt% active Ti and inactive SiC particulate added CMCs prepared from PPS at various temperatures, respectively. The results showed that with the use of active fillers formation of the new phases; TiC, TiSi and TiO within the amorphous matrix occurred due to the reactions between the Ti and decomposition products of the polymer.

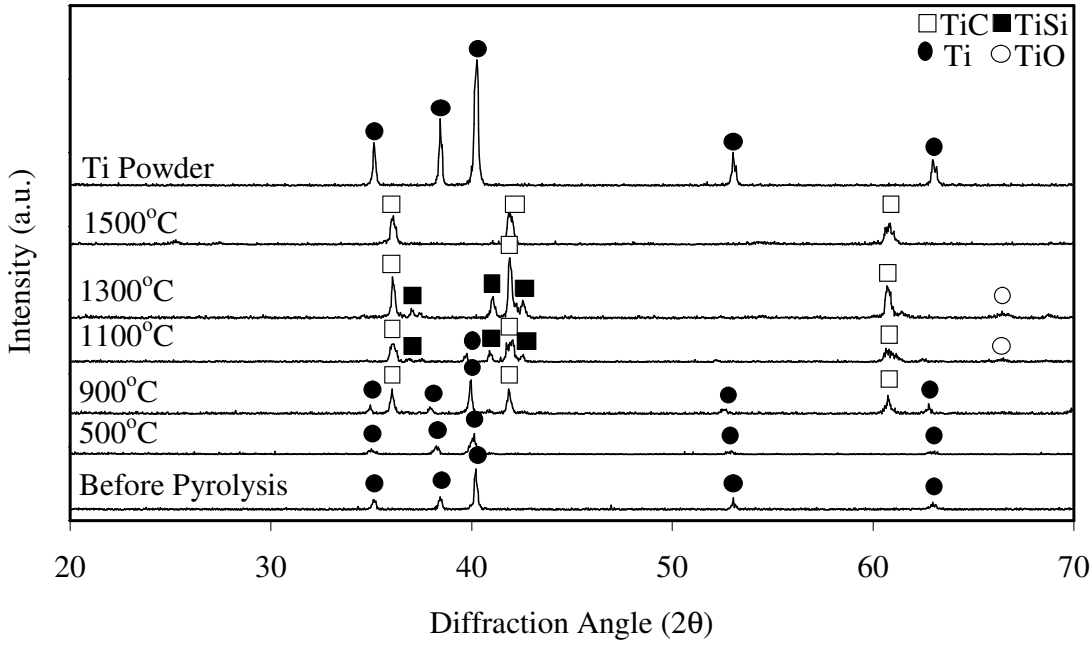


**Figure 5.8** X-ray diffraction patterns of 60 wt% Ti /PPS pyrolyzed under Ar at various temperatures.

Pyrolysis temperature is the most critical parameter in the formation of new phases. Up to 500°C, Ti peaks were observed. At 900°C, the formation of TiC was detected. With increasing the pyrolysis temperatures the peak intensities of the TiC phase get higher. 1100°C was critical temperature in the formation of TiSi. This silicate phase was observed up to 1300°C. At around 1500°C, formation of TiC was significant. Figure 5.9 shows the XRD patterns for composite system with inert filler (SiC / PPS system). As seen in the figure no new phase development was observed in the case of inert SiC particulate addition.

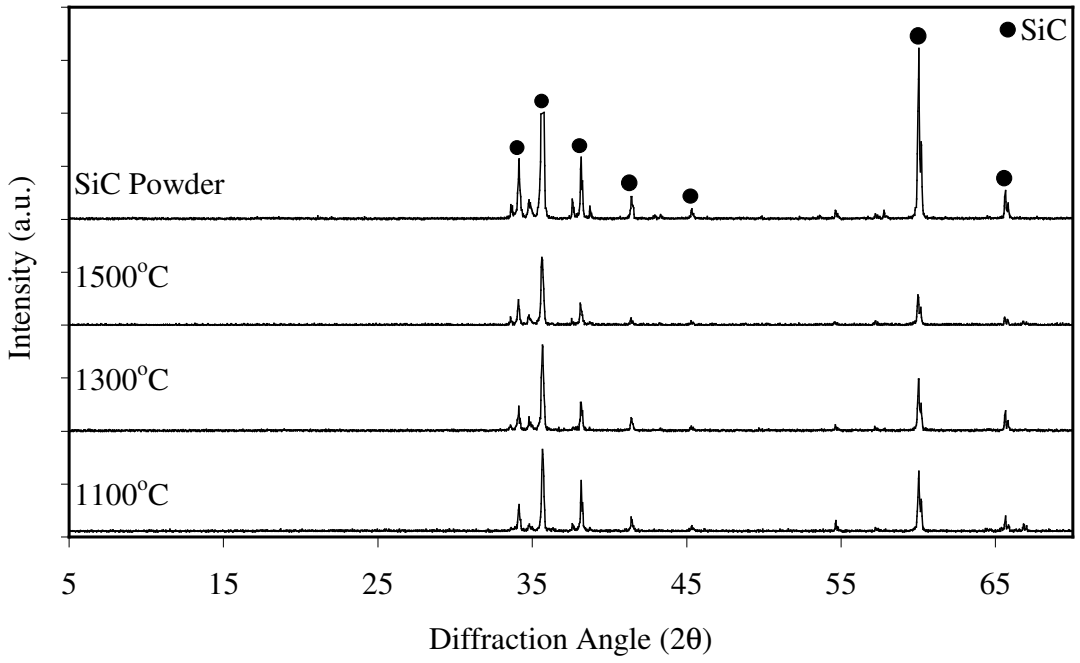


**Figure 5.9** X-ray diffraction patterns of 60 wt% SiC /PPS pyrolyzed under Ar at various temperatures.

Figure 5.10 shows the XRD patterns of samples prepared with 80wt% Ti addition into PPS polymer. Increasing the weight fraction of the active fillers yielded the similar phases as compared to low fractions.

Pyrolysis atmosphere has significant effect on the pyrolysation of CMCs and formation of new phases and microstructural properties. Figure 5.11 shows the XRD pattern of 80wt% Ti added PPS samples pyrolyzed at elevated temperatures under $N_2$ atmosphere. Under $N_2$ atmosphere, no TiO formation was observed, however TiN formation occurred and its intensity increased with increase in pyrolysis temperature. At low temperatures (900°C) TiC and TiSi phases were detected. TiN phase was also detected with very low intensity. At higher temperatures the intensity of the TiN increases significantly.

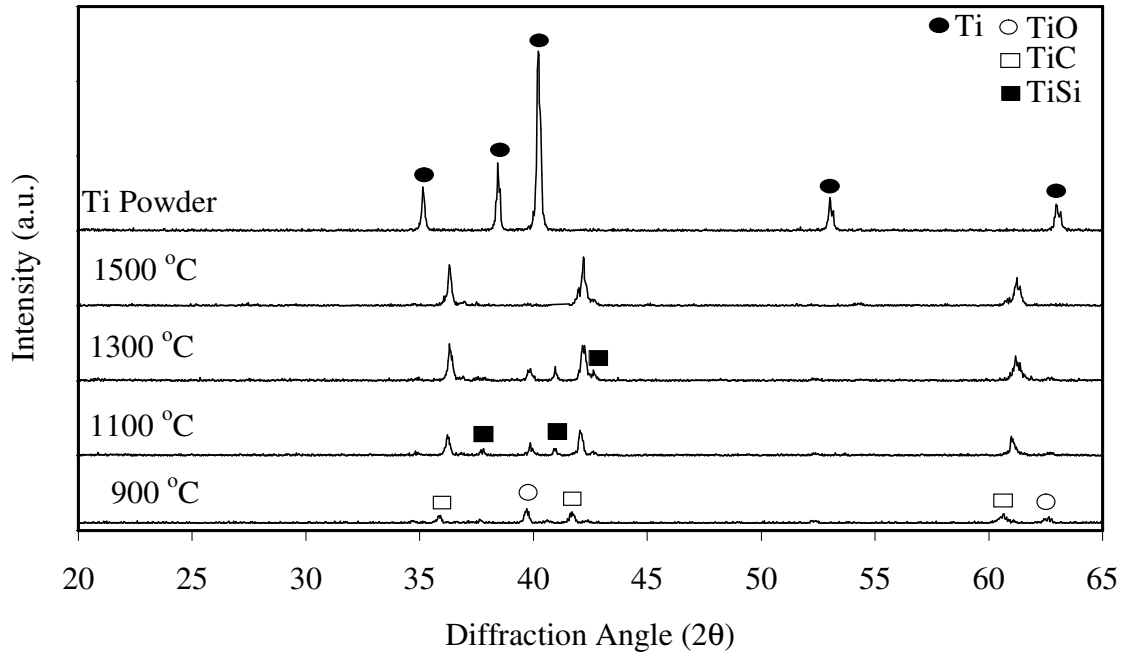


**Figure 5.10** X-ray diffraction patterns of 80 wt% Ti /PPS pyrolyzed under Ar at various temperatures.

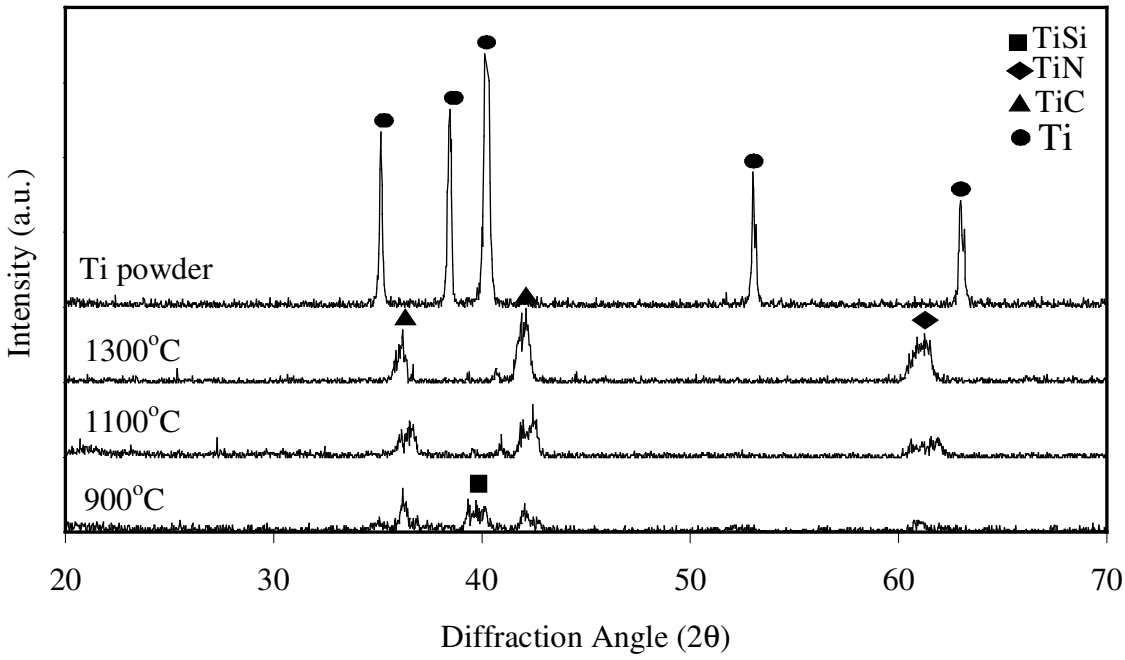


**Figure 5.11** X-ray diffraction patterns of 80 wt% Ti /PPS pyrolyzed under $N_2$ at various temperatures.

To monitor the effect of the polymer type on the microstructural development, composite specimens with PMS precursor were prepared in addition to the samples with PPS. Figure 5.12 shows the XRD patterns of the 60wt% Ti added CMC monoliths prepared from PMS at various temperatures. Similar to PPS, pyrolysis of Ti/PMS green bodies yields the formation of TiC, TiSi and TiO phases. Samples pyrolyzed at temperatures lower then 1500°C showed the formation of TiO, TiC and TiSi phases at 1500°C only TiC phases was observed. The phase developments were also monitored using SEM-EDX analysis. As an example, fracture surface SEM image of 80wt% Ti filled CMC prepared at 900°C from Ti/PMS bodies was shown in Figure 5.13. On this image, elemental distributions along the line A to E were given in Table 5.2. As seen from the table, regions A and E are Ti rich and a matrix region with some compositional gradients may form between the adjacent Ti particulates. The matrix may consist of the decomposition products of the preceramic polymers and their reaction with Ti powder. Region B and D may compose of TiO, TiSi and TiC while Region C is SiOC rich phases.

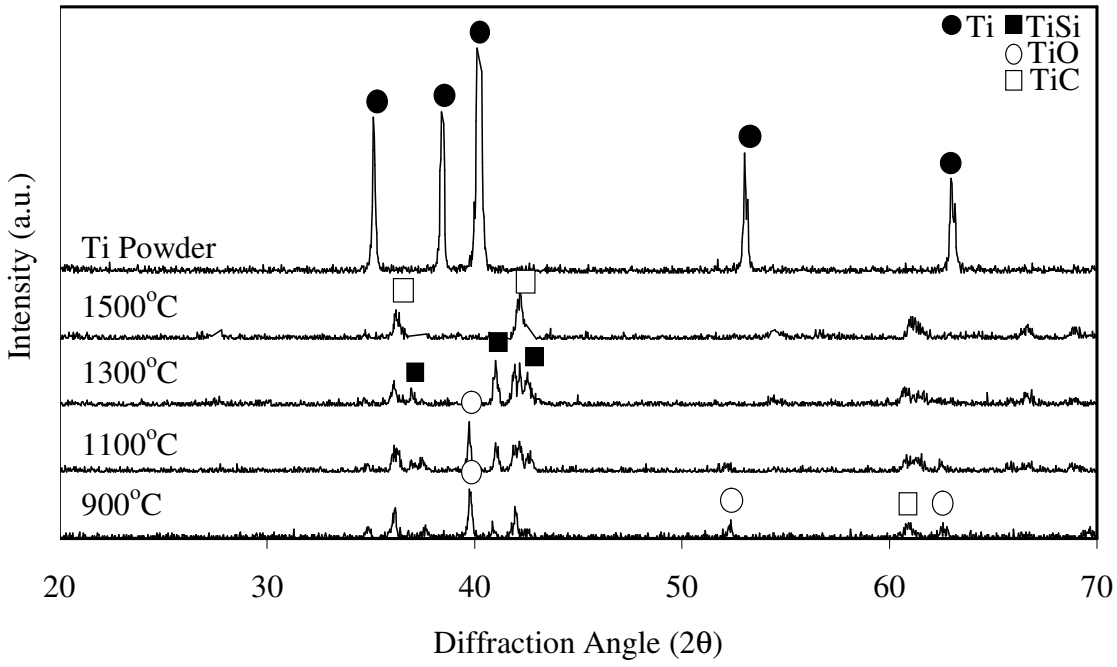


**Figure 5.12** X-ray diffraction patterns of 60 wt% Ti /PMS pyrolyzed under Ar at various temperatures.

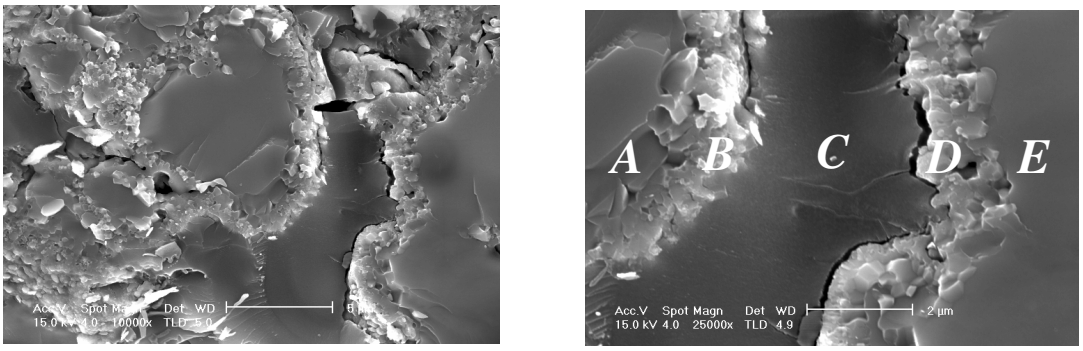


(a) (b)

**Figure 5.13** Fracture surface SEM micrograph of 80wt% Ti filled CMC monolith prepared from Ti/PMS bodies at 900°C.

**Table 5.2** Elemental distributions along the line between two adjacent Ti rich particulates for 80 wt% Ti filled CMC monolith prepared from Ti/PMS bodies at 900°C.

| *Region* | *C wt%* | *Si wt%* | *Ti wt%* | *O wt%* |
|---|---|---|---|---|
| **A** | 3 | 4 | 82 | 11 |
| **B** | 3 | 17 | 44 | 36 |
| **C** | 5 | 47 | 7 | 41 |
| **D** | 4 | 12 | 71 | 13 |
| **E** | 2 | 1 | 80 | 17 |

On the other hand, at pyrolysis temperatures above 1100°C, these distinct phases cannot be detected evidently, as shown in Figure 5.14. At elevated temperatures, compositional gradients and also the interphases may diminish due to extensive reaction/diffusion of the filler and pyrolysis products as can be followed from the EDX analysis shown in Table 5.3. This may give more homogeneous distribution of the elements in the ceramic structure. As shown in Figure 5.14 (a) samples pyrolyzed at 1100°C still show distinct phase distributions region (A and D are Ti rich and Si poor, B and C may be composed of TiO, TiSi and TiC). However Figure 5.14 (b) and (c) show more homogenous distribution of Ti and other elements.

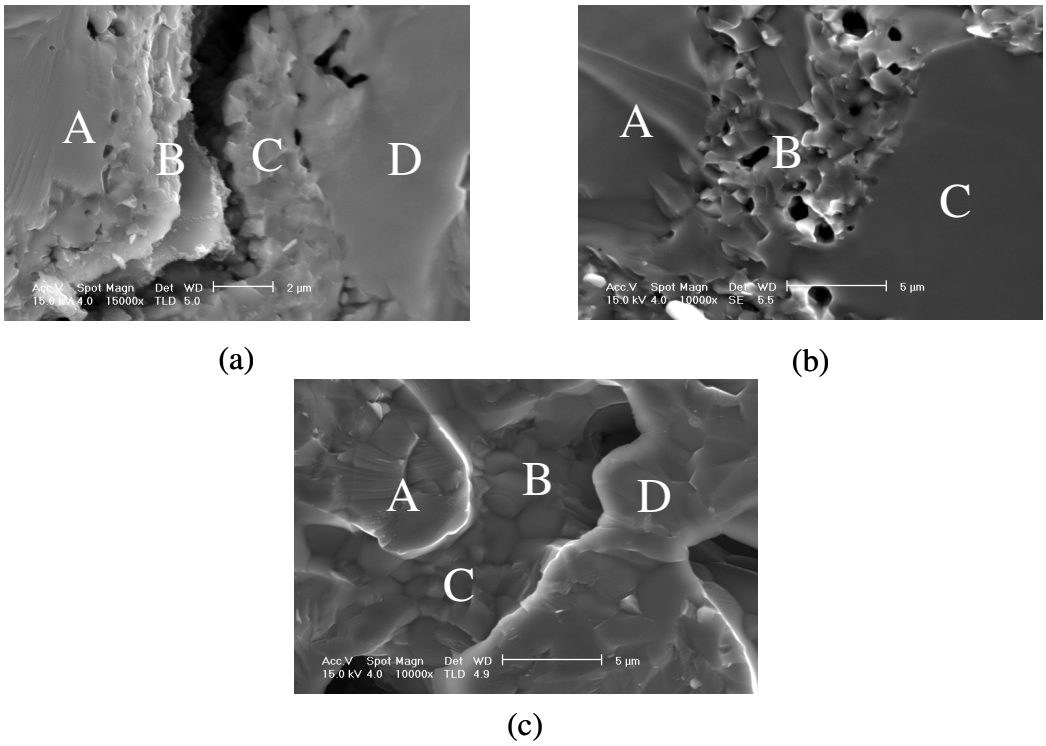


**Figure 5.14** Fracture surface SEM micrograph of 80wt% Ti filled CMC monolith prepared from Ti/PMS bodies at (a) 1100°C (b) 1300°C (c) 1500°C.

**Table 5.3** Elemental distributions at different regions of samples shown in Figure 5.14.

| *Sample* | *Region* | *C wt%* | *Si wt%* | *Ti wt%* | *O wt%* |
|---|---|---|---|---|---|
| **(a)** | **A** | 2 | 1 | 81 | 17 |
| | **B** | 2 | 19 | 57 | 22 |
| | **C** | 9 | 6 | 68 | 18 |
| | **D** | 2 | 1 | 75 | 22 |
| **(b)** | **A** | 2 | 0.25 | 90 | 8 |
| | **B** | 2 | 3 | 90 | 5 |
| | **C** | 2 | 0.3 | 88 | 10 |
| **(c)** | **A** | 1 | 24 | 65 | 9 |
| | **B** | 6 | 0.4 | 73 | 21 |
| | **C** | 1 | 25 | 63 | 11 |
| | **D** | 2 | 0.4 | 74 | 23 |

### 5.3 Thermal Transformations, Ceramic Yield and Mass Losses

Pyrolytic conversions of polymeric precursor into Si-O-C systems may lead to the formation of gaseous products that causes weight losses, volumetric changes and formation of micro cracks due to shrinkages and finally a deterioration of mechanical properties. Figure 5.15 and 5.16 show the weight changes of the neat and active Ti added PPS and PMS samples pyrolyzed at various pyrolysis temperatures. For pyrolysis in the range of 900-1500$^{o}$C, phenyl containing precursor, PPS lose its weight of 15-17 %, while methyl containing precursor PMS lose 22-27 % of the weight, respectively. This is due to the highest carbon content of PPS precursor.

Weight changes are considerably affected by the incorporation of active Ti fillers into ceramic structure. This is due to the reduction of the polymer ratio in the green composite and the reactions between the decomposition products of the polymer and filler particles. Incorporation of Ti fillers into PPS polymers reduced weight change values to about 2%. Filler ratio also affects the weight change values of the Ti / PPS systems. However in the Ti / PMS system the filler ratio doesn't have a considerable effect on weight change values, but addition of Ti also reduced the values from 17% to 1.5%.

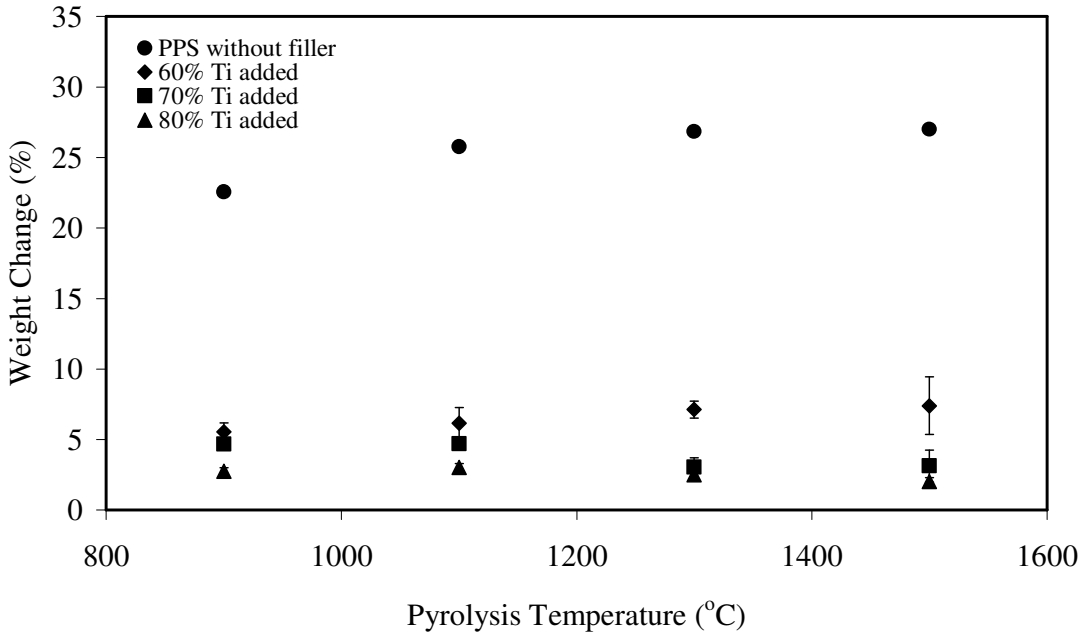


**Figure 5.15** Weight changes values as a function of pyrolysis temperature for samples of 0, 60, 70, 80 wt% Ti added PPS.

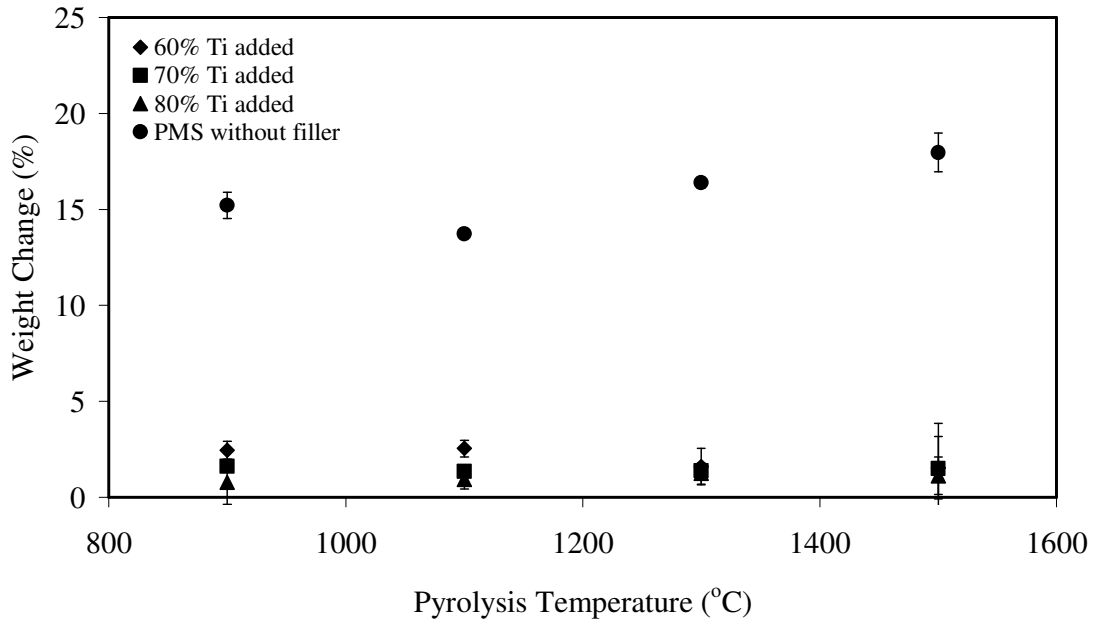


**Figure 5.16** Weight changes values as a function of pyrolysis temperature for samples of 0, 60, 70, 80 wt% Ti added PMS.

Figure 5.17 shows the weight change values of Si / PPS system. Si addition also affects the weight change values considerably, and in this system the effect of filler ratio is much evident. For example with the addition of 60 wt% Si weight changes values were about 10 %, with the addition of 70 wt% about7 %, and with the addition of 80 wt% about 5% at 1300°C. Addition of inactive fillers into the polymers shows the same effects on weight change values with active filler addition. Figure 5.17 shows the weight change values of SiC/PPS system. Here, also the effect of filler ratio was followed. Weight change values decreased with increasing filler ratio.

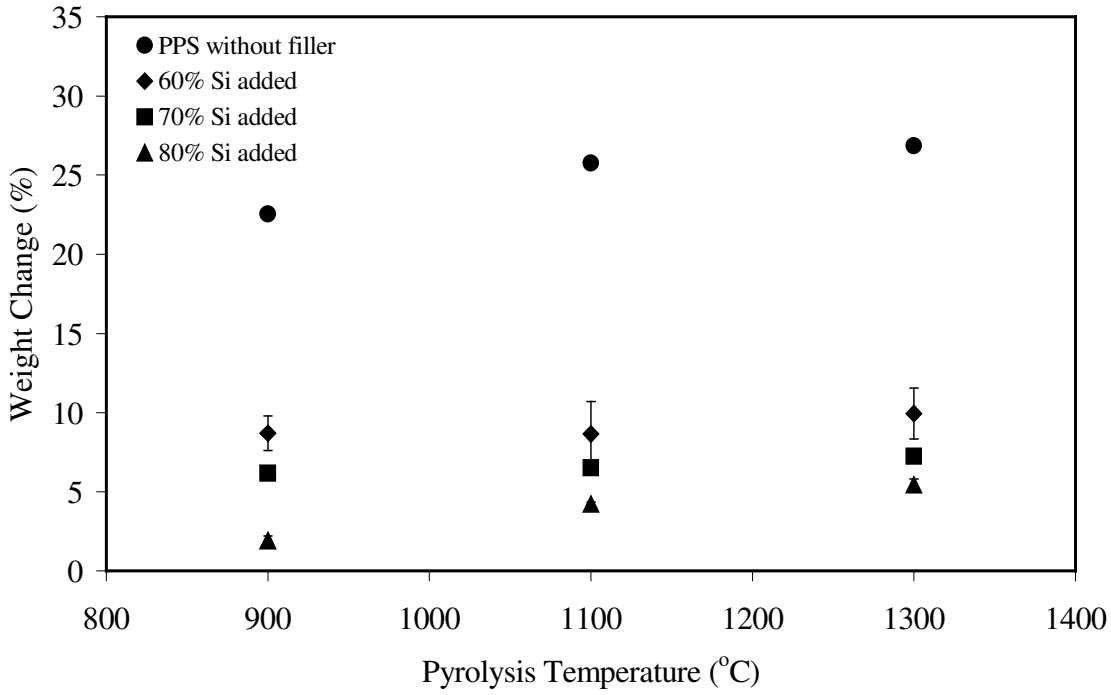


**Figure 5.17** Weight change values as a function of pyrolysis temperature for samples of 0, 60, 70, 80 wt% Si added PPS.

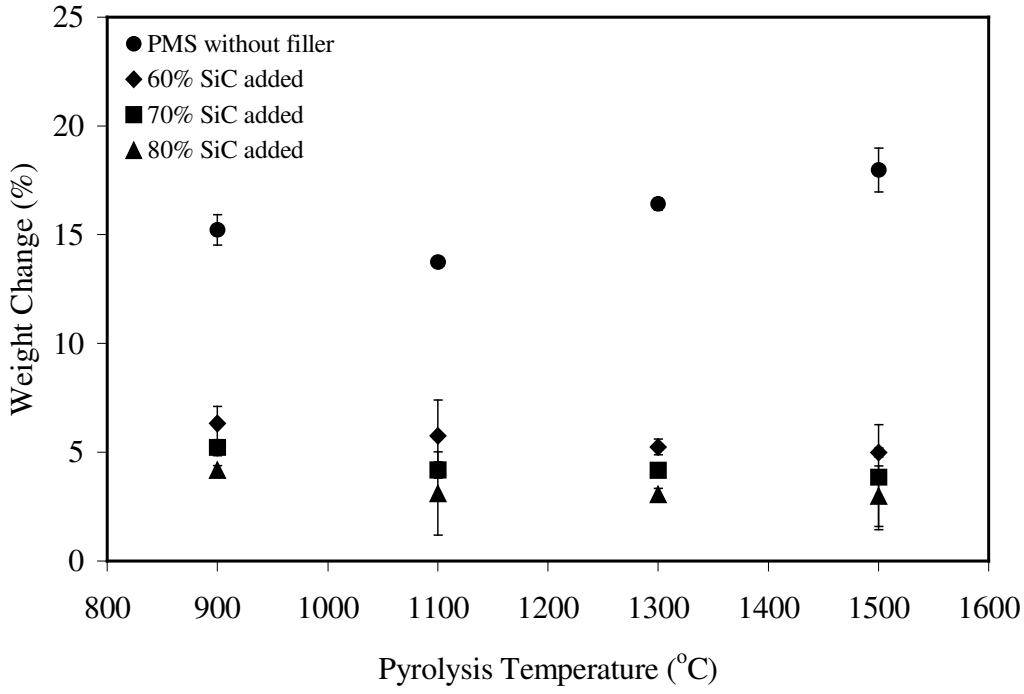


**Figure 5.18** Weight change values as a function of pyrolysis temperature for samples of 0, 60, 70, 80 wt% SiC added PMS.

Differences in the microstructure between active and inert filler added samples after pyrolyzation can be easily observed with SEM analysis. In Figure 5.19 fracture surface SEM micrographs of samples prepared with addition of active Ti and inert SiC powders into PPS precursor are seen after pyrolyzation under 1300°C. It is apparent that adhesion of polymer and filler particles is better in active filler containing composites than that of inert filler ones. Also, in Ti added samples a structure with continuity is observed as compared to those with SiC particles. The microstructural feature of the samples is expected to affect the mechanical properties.

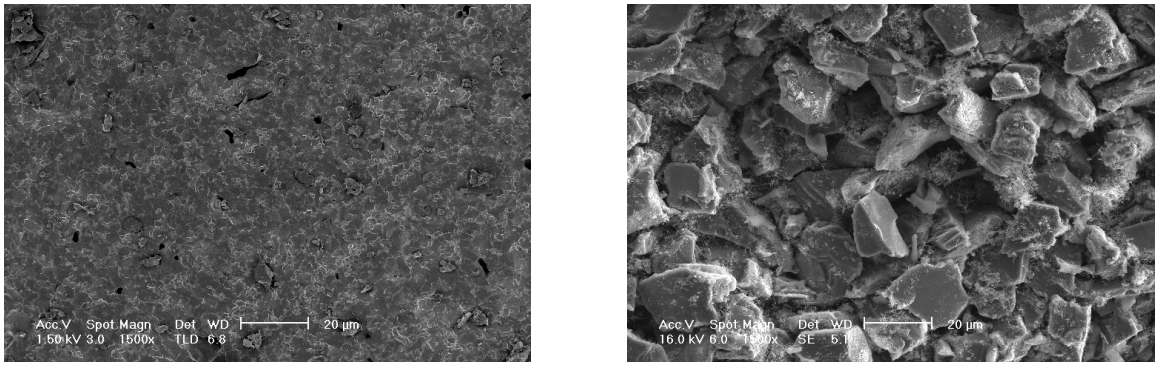


(a) (b)

**Figure 5.19** Fracture surface SEM micrograph of (a) 80wt% Ti (b) 80 wt% SiC filled PPS precursor pyrolyzed at 1300°C.

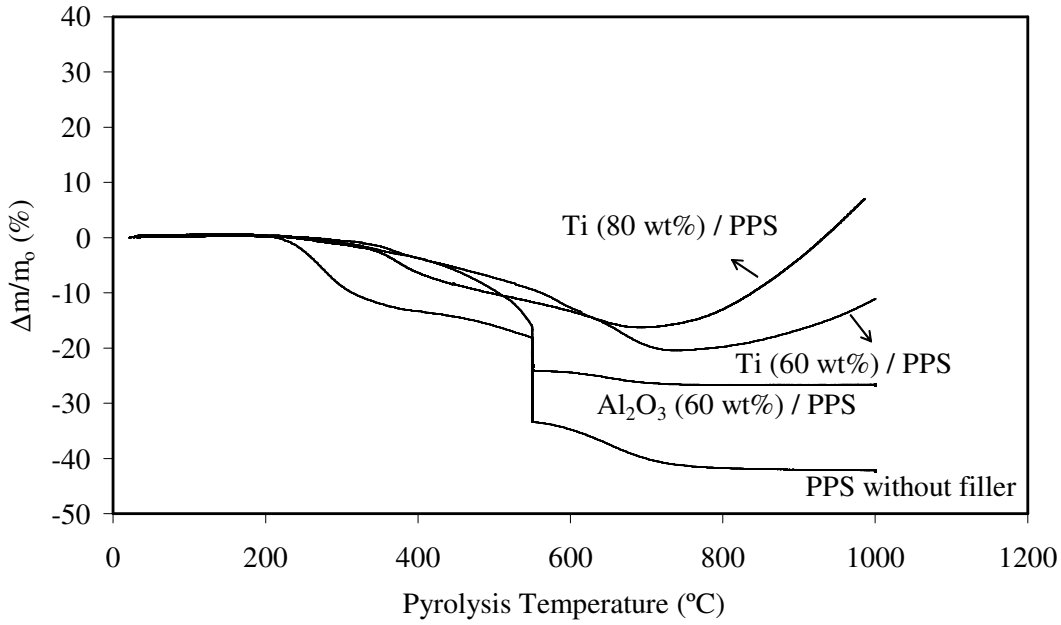


**Figure 5.20** TGA micrographs of without filler addition, 80wt% Ti, 60 wt% of Ti and 60 wt%$Al_2O_3$ filled PPS precursor pyrolyzed up to 1300°C under $N_2$ atmosphere.

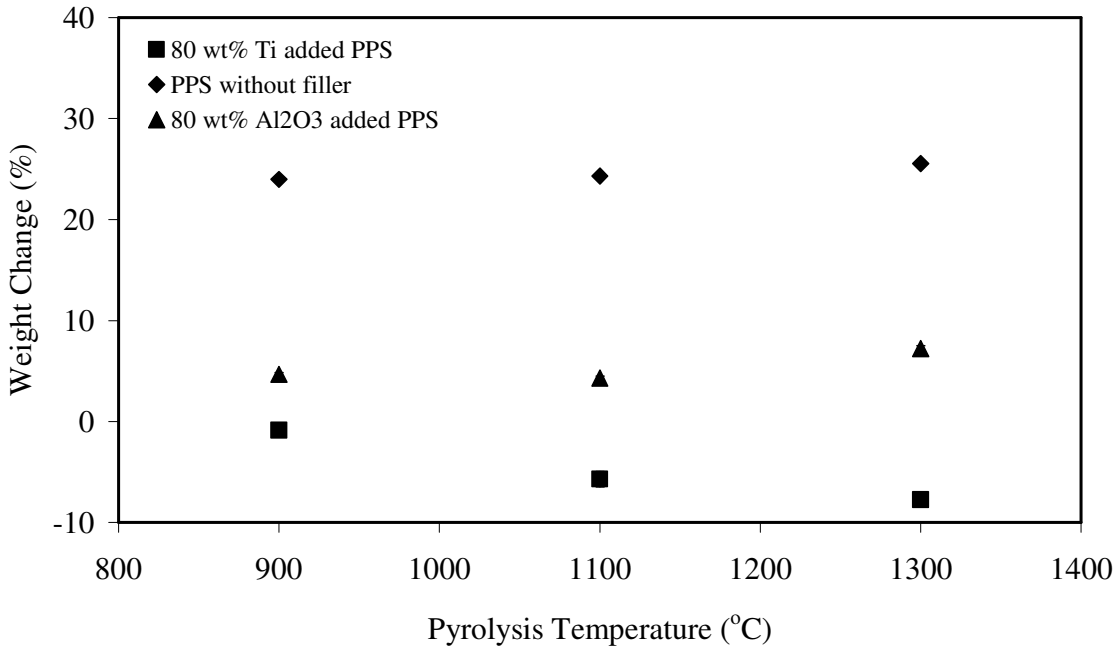


**Figure 5.21** Weight change values as a function of pyrolysis temperature for samples of PPS without filler addition and 80 wt% Ti and $Al_2O_3$ added PPS pyrolyzed under $N_2$ atmosphere.

As seen in Figure 5.20, TGA analysis showed that the mass loss of the samples starts at 500°C which is the decomposition temperature of the polymer. Neat polymer loses 41.2% of its weight at 1000°C. Addition of the fillers decreases the weight loss ratio depending on the decrease in the polymer ratio. In 60 wt% $Al_2O_3$ added samples, weight loss value was about 25%. By the addition of active fillers, the weight loss was minimum and by pyrolysis above 800°C a weight gain was monitored. This may be due to the reactions between filler particles and reactive gas atmosphere ($N_2$). Figure 5.21 that shows the weight change of the samples pyrolyzed in tubular furnace confirms the weight gains observed in TGA with pyrolysis under $N_2$ atmosphere. Addition of inert $Al_2O_3$ reduces the weight change ratio, however, active filler added samples show weight gain values above 900°C. Polymer to ceramic conversions may also lead to an increase in the density and the resulting densification may result in the formation of cracks in the microstructure of the pyrolysis product. Densification during organic to inorganic conversion can be controlled by incorporation of the active fillers by reducing the polymer ratio and promoting the reactions between the polymer decomposition products and the filler particles to control the shrinkage, porosity formation and

microcracking. Effects of the type of the polymer and pyrolysis temperature on the final densities of the ceramic monoliths made with PPS and PMS are shown in Figures 5.22 and 5.23, respectively. The density of the green bodies was measured in the range of 2-2.7 g/cm$^3$ before pyrolysis. The highest density values for CMCs were obtained with addition of 80wt% Ti (4.689 g/cm$^3$) in PPS samples, however, the effect of the filler ratio in PMS samples were found to be negligible. Density values of the PPS samples increase with increasing pyrolysis temperature, while 1100$^o$Cwas found to be optimum point for PMS.

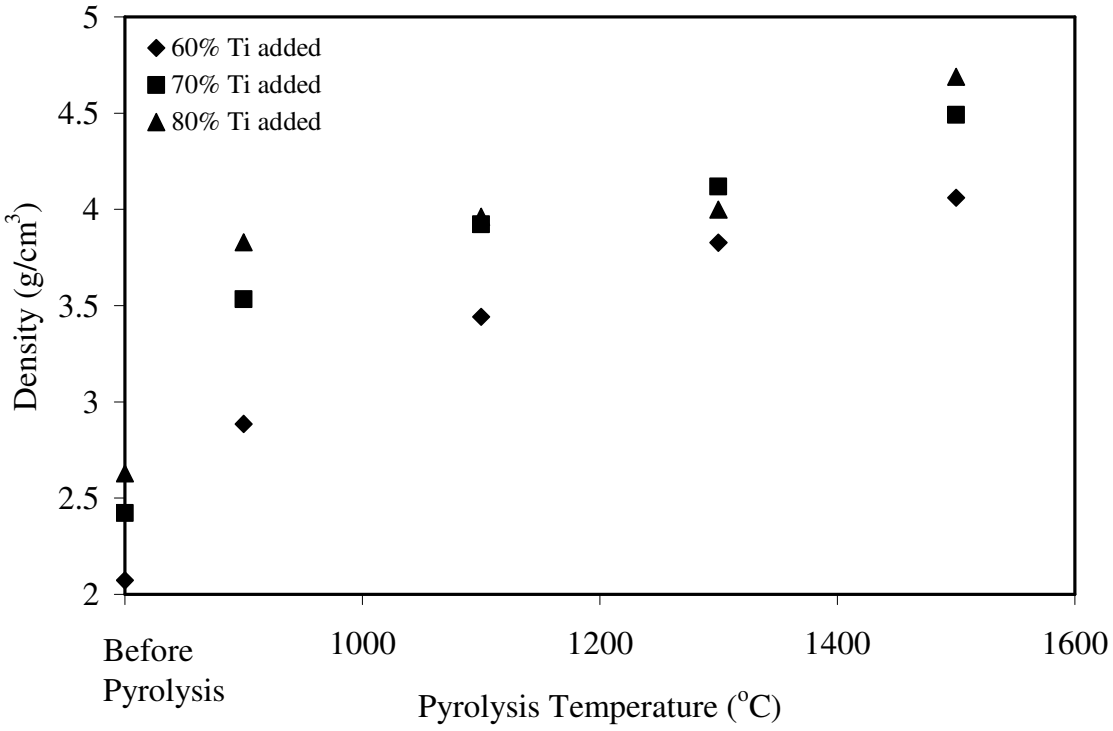


**Figure 5.22** Density values for the samples prepared with addition of 60, 70, 80wt% Ti into PPS as a function of pyrolysis temperature.

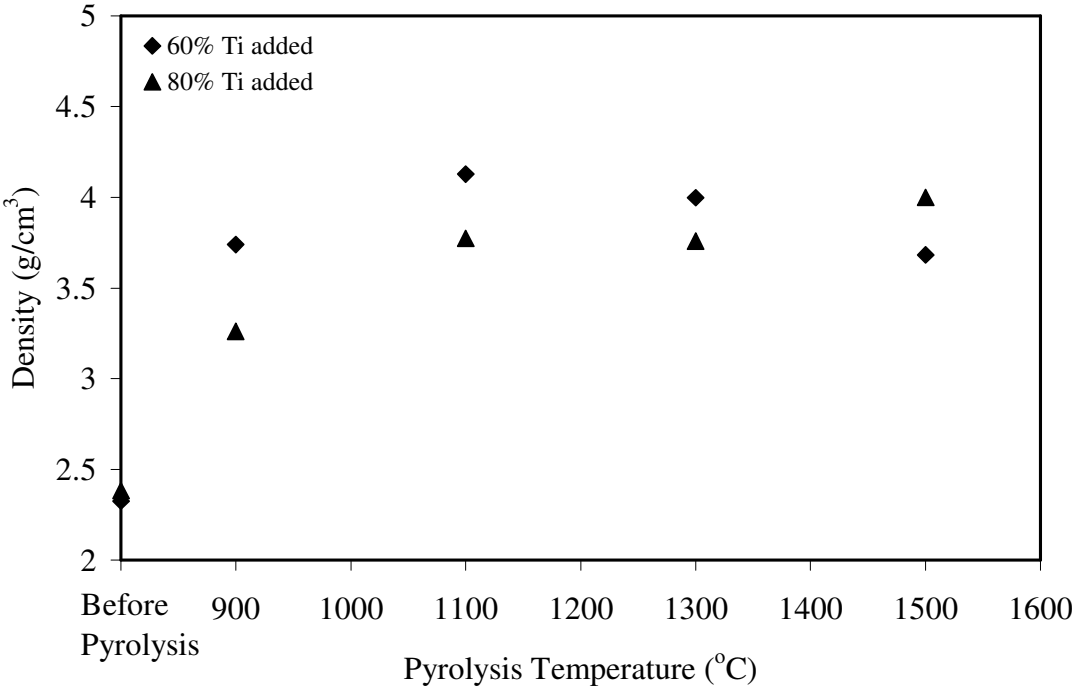


**Figure 5.23** Density values for the samples prepared with addition of 60 and 80wt% Ti into PMS as a function of pyrolysis temperature.

The effect of the filler type on density changes was also measured. Density values of 80 wt% active (Ti, Si) and inert (SiC, $Al_2O_3$) filler added PPS samples are shown in Figure 5.24. Density values of some metals and ceramics are also given in Table 5.3 for comparison. As seen from the table the density of Ti metal is 4.5 g/cm$^3$ and TiC ceramic is 4.94 g/cm$^3$. The measured value at 900$^o$C for Ti added samples is 3.83 g/cm$^3$ and this value reached up to 4.7 g/cm$^3$ at 1500$^o$C because of the formation of TiC phases in the structure. Also, addition of 80 wt% Si powder gives very low density values of about 2 g/cm$^3$, because of the low density of Si powder (1.5 g/cm$^3$).

**Table 5.4** Density values of some metals and ceramics [46].

| **Material** | **Density (g/cm$^3$)** |
|---|---|
| Ti | 4.5 |
| TiC | 4.94 |
| Si | 1.5 |
| SiC | 3.2 |
| $Al_2O_3$ | 3.96 |
| Glass | 2.6 |

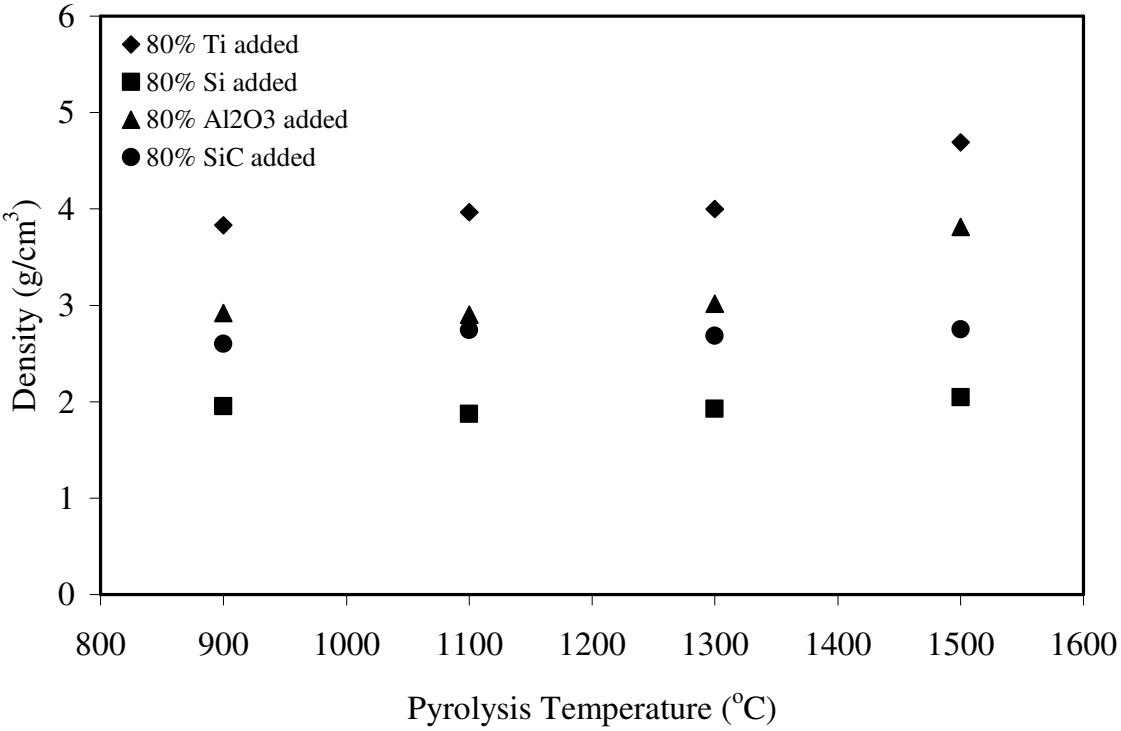


**Figure 5.24** Density values for the samples prepared with addition of 80wt% Ti, Si, SiC, and $Al_2O_3$ into PPS as a function of pyrolysis temperature.

Polished surface SEM images for CMCs made with 80 wt% Ti filled PPS and PMS polymers pyrolyzed at various temperatures are illustrated in Figures 5.25 and 5.26, respectively. As seen in the figures, as the pyrolysis temperatures increases a reduction of porosity is observed for PPS, while pore fraction increases for PMS made composites. This is in agreement with density values of these samples. For PPS samples the density values increases with increasing temperature and poreless samples were formed, however in PMS samples at 1500°C pore formations increased and low density samples were formed.

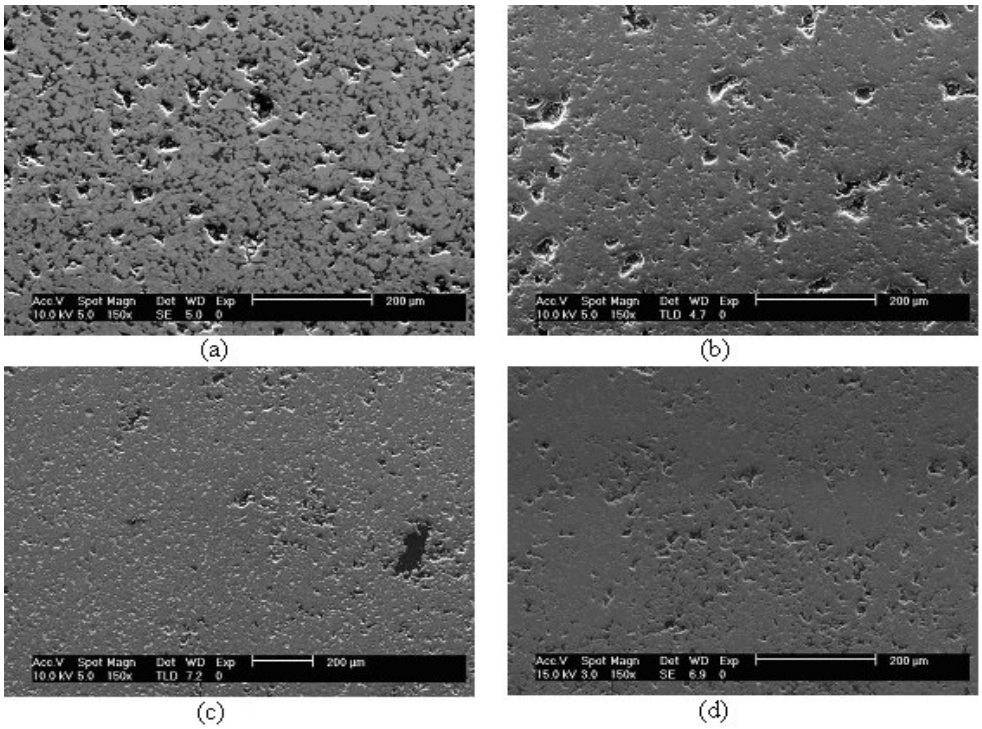


**Figure 5.25** SEM polished surface micrographs of 80 wt% active Ti filled PPS pyrolyzed at various temperatures (a) 900, (b) 1100, (c) 1300, (d) 1500°C.

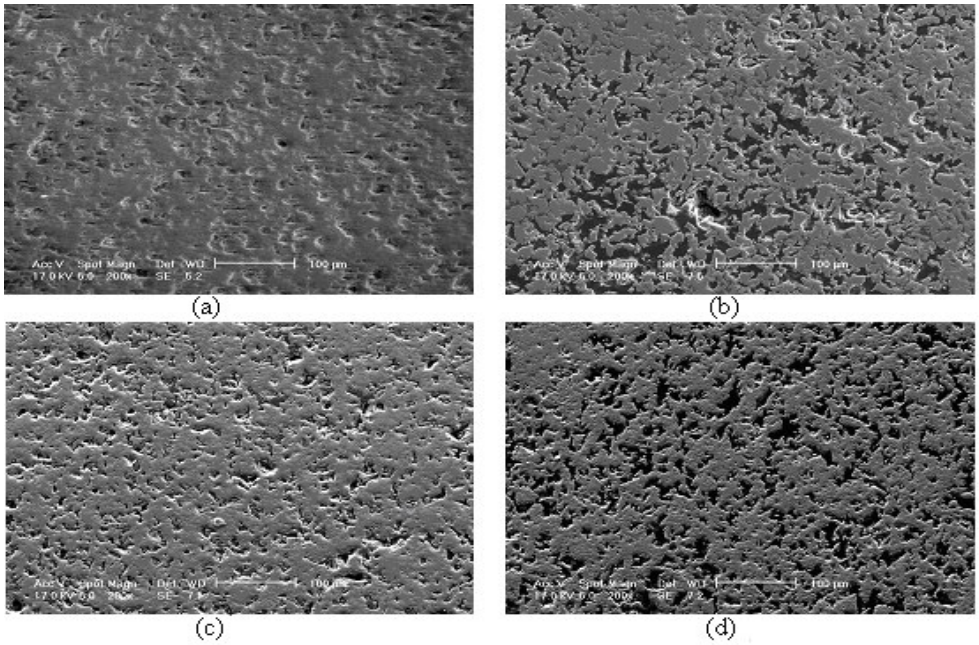


**Figure 5.26** SEM polished surface micrographs of 80 wt% active Ti filled PMS pyrolyzed at various temperatures (a) 900, (b) 1100, (c) 1300, (d) 1500°C.

### 5.4 Mechanical Behavior of SiOC Based Composites

Hardness tests were carried out to evaluate the effects of pyrolysis temperature and filler addition into the polymers on the mechanical behavior of the composites. Figure 5.27 and 5.28 shows the hardness values of ceramics without filler addition and Ti added PPS and PMS samples, respectively. It was found that neat ceramics reach the maximum hardness values (8.88 GPa for neat PPS, 10.67 GPa for neat PMS) at 1100$^{o}$C, which is the optimum temperature for crack free samples with the least amount of porosity. However, the polymers exhibited distinct behavior by the incorporation of Ti particulates. For PPS, at low concentrations and pyrolysis temperatures, the addition of Ti reduced the hardness values, however, at concentrations above 70 wt% resulted in the higher values (up to 13.20 ±2.05 GPa) as compared with those with neat polymer. On the other hand, for PMS, addition of Ti reduced the hardness of composites for all concentrations.

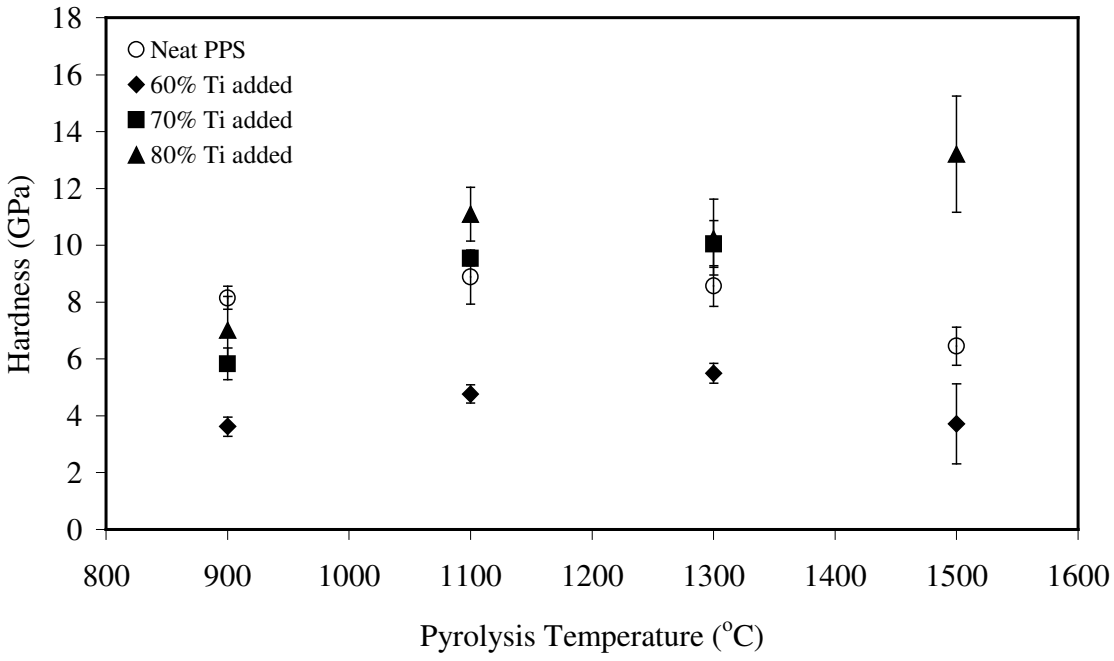


**Figure 5.27** Vickers hardness values as a function of pyrolysis temperature for neat ceramics and composites made with various Ti added PPS precursor.

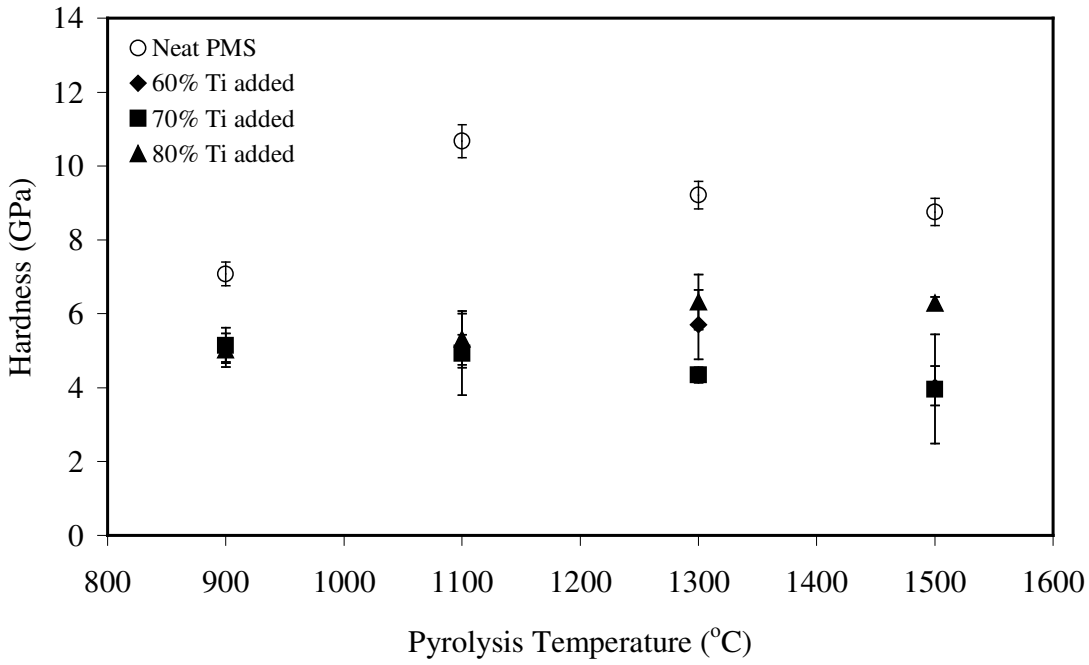


**Figure 5.28** Vickers hardness values as a function of pyrolysis temperature for neat ceramics and composites made with various Ti added PMS precursor.

Table 5.4 shows Vickers hardness values of some advanced ceramic structures for comparison. It is seen from the table that glasses have the hardness values between 5-10 GPa. When compared with this neat PPS and PMS samples, which have the hardness values of about 9 GPa and 11 GPa at 1100°C, respectively gives very comparable results. After addition of Ti powder these values reach up to 14 GPa in PPS samples depending on the microstructure, which is very close to the values of aluminas and silicon nitrides.

**Table 5.5** Vickers hardness values of some ceramic structures.

| **Material Class** | **Vickers Hardness (HV) GPa** |
|---|---|
| Glasses | 5 – 10 |
| Zirconias, Aluminium Nitrides | 10 - 14 |
| Aluminas, Silicon Nitrides | 15 - 20 |
| Silicon Carbides, Boron Carbides | 20 - 30 |
| Cubic Boron Nitride CBN | 40 - 50 |
| Diamond | 60 – 70 > |

# CHAPTER 6
# CONCLUSIONS

Active and inert filler incorporated ceramic composites were developed based on the pyrolytic conversion of – phenyl and – methyl containing polysiloxanes. This study focused on investigating the effect of filler type and ratio, pyrolysis temperature and atmosphere on the phase development and mechanical properties of the SiOC based ceramic matrix composites. X-ray diffraction (XRD) measurements revealed that the thermal transformation of the polymers without filler yielded amorphous silicon oxycarbide ($SiO_xC_y$) ceramics at temperatures below 1300$^oC$, however, at higher temperatures (~1500$^oC$) crystalline β-SiC phases formed. At pyrolysis temperatures above 900$^oC$, the release of volatiles such as hydrocarbons occurs by the decomposition of the preceramic polymers. This was confirmed by Fourier Transform Infrared (FTIR) studies. SiOC phase formations were also confirmed with SEM-EDX analysis performed on fracture surfaces of neat ceramic samples. The decompositions of the polymers and release of hydrocarbons resulted with shrinkage and porosity formations. SEM micrographs of neat poly(phenyl)siloxane (PPS) samples shows that formation of pores increased with increasing pyrolysis temperature, however no pore formations observed in poly(methyl)siloxanes (PMS). This may be the result of the different methyl containing structure of the precursor.

Active (Ti and Si) and inert (SiC and $Al_2O_3$) fillers were added into the polymers to compensate the negative mass loss and shrinkage effect due to the decomposition of the polymers. Inert fillers compensate the mass losses by decreasing the polymer ratio. Active fillers however, compensate the mass losses with both decreasing the polymer ratio and with reaction of active filler and decomposition products of the polysiloxanes. XRD analysis revealed that TiC, TiSi and TiO phases formed within the amorphous matrix due to the reactions between the active Ti particulates and the polymers, however addition of inert SiC resulted with no new phase formations. Pyrolysis of the samples under reactive $N_2$ atmosphere also yielded new phases such as TiN.

Effect of the thermal transformations on the mass loss and density values was also measured and found that they are considerably affected by the addition of fillers. Neat PPS samples show weight loss values about 25% while PMS polymer shows 17%. This may be due to the highest carbon content of phenyl containing PPS polymer.

Incorporation of active and inert fillers decreases these values nearly to 2%. Filler ratio also effects the weight change values of the CMCs. The results imply that pyrolysis temperature has some significant effect on the densification behavior. The highest density values for CMCs were obtained with the addition of 80 wt% Ti in PPS samples, however, the effect of the filler ratio in PMS samples were found to be negligible and a decrease in density values was observed with increasing pyrolysis temperature in Ti/PMS systems. These results were confirmed by the SEM polished surface micrographs of the Ti added PPS and PMS samples. At higher pyrolysis temperatures the formation of pores was detectable in Ti/PMS samples while a relatively smooth surface was observed in Ti/PPS systems.

The polymers exhibited distinct mechanical behavior by the incorporation of Ti particulates. Unfilled samples gave the maximum hardness values at 1100$^{o}$C which is the optimum temperature for crack free samples with least amount of porosity. Maximum hardness values for the neat samples are comparable with conventional glasses (~10GPa). With addition of Ti into PPS increased the hardness values with increasing the filler ratio and reached to ~14GPa which is very close to the hardness of aluminas and silicon nitrides. However, addition of filler into PMS polymer decreases hardness values for all compositions and this is in agreement with microstructural features of the samples.

# REFERENCES


[1] Parmentier J., Soraru G. D., Babonneau F., "Influence of the Microstructure on the High Temperature Behavior of Gel-Derived SiOC Glasses", *J. Eu. Ceram. Soc.* 21 (2001) 817-824

[2] Mutin P .H., "Control of the Composition and Structure of Silicon Oxycarbide and Oxynitride Glasses Derived from Polysiloxane Precursors", *J. Sol-Gel Sci. Tech.* 14 (1999) 27-38

[3] Harshe R., Balan C., Riedel R, "Amorphous Si(Al)OC Ceramic from Polysiloxanes: Bulk Ceramic Processing, Crystallization Behavior and Applications", *J. Eu. Ceram. Soc.* V:24 I:12 (2004) 3471-3482

[4] Walter S., Soraru G. D., Brequel H., Enzo S., "Microstructural and Mechanical Characterization of Sol-Gel Derived Si-O-C Glasses", *J. Eu. Ceram. Soc.* 22 (2002) 2389-2400

[5] Greil P., "Near Net Shape Manufacturing of Polymer Derived Ceramics", *J. Eu. Ceram. Soc.* 18 (1998) 1905-1914

[6] Kaindl A., Lehner W., Greil P., Kim D. J., "Polymer-Filler Derived $Mo_2C$ Ceramics", *Mat. Sci. and Eng.* A260 (1999) 101-107

[7] Greil P., "Near Net Shape Manufacturing of Ceramics", *Mat. Chem. Phys.* 61 (1999) 64-68

[8] Michalet T., Parlier M., Addad A., Duclos R., Crampon J., "Formation at Low Temperature with Low Shrinkage of Polymer/Al/$Al_2O_3$ Derived", *Ceram. Int.* 27 (2001) 315-319

[9] Soraru G. D., Kleebe H. J., Ceccato R., Pederiva L., "Development of Mullite-SiC Nanocomposites by Pyrolysis of Filled Polymethylsiloxane Gels", *J. Eu. Ceram. Soc.* 20 (2000) 2509-2517

[10] Schiavon M. A., Radovanovic E., Yoshida I. V. P., "Microstructural Characterisation of Monolithic Ceramic Matrix Composites from Polysiloxane and SiC Powder", *Pow. Tech.* 123 (2002) 232-241

[11] Michalet T., Parlier M., Beclin F., Duclos R., Crampon J., "Elaboration of Low Shrinkage Mullite by Active Filler Controlled Pyrolysis of Siloxanes", *J. Eu. Ceram. Soc.* 22 (2002) 143-152

[12] William D., Callister J. R., "*Materials Science and Engineering, An Introduction*"; published by John Wiley and Sons, (1991)

[13] Jones J. T., Benard M. F., "*Ceramics Industrial Processing and Testing*", Iowa State University Press, (1993)

[14] Liang Y., Dutta S. P., "Application Trend in Advanced Ceramic Technologies", *Technovation* 21 (2001) 61-65

[15] Somiya S. "*Advanced Technical Ceramics*", Academic Press, (1989)

[16] Kingery W. D., Bowen H. K., Uhlmann D. R., "*Introduction to Ceramics*", Wiley-Interscience Press, (1976)

[17] Barsoum M. "*Fundamentals of Ceramics*", Iop Institute of Physics, (2003)

[18] Reed J. S., "*Principals of Ceramic Processing*", Wiley-Intersicence Press, (1995)

[19] Brinker C. J., Scherer G. W., "*Sol-Gel Science-The Physics and Chemistry of Sol-Gel Processing*", New York, Academic Press, (1990)

[20] Schiavon M. A., Redondo S. U. A., Pina S. R. O., Yoshida I. V. P., "Investigation on Kinetics of Thermal Decomposition in Polysiloxane Networks Used as Precursors of Silicon Oxycarbide Glasses", *J Non-cryst. Solids.* 304 (2002) 92-100

[21] Kawamura K., Kaga J., Iwata T., Yamanaka S., Ono M., "Silicon Carbide Coating on Alumina Film Using Polycarbosilane", 99 [1] (1991) 94-96

[22] Goerk O., Feike E., Heine T., Trampert A., Schubert H., "Ceramic Coatings Processed by Spraying of Siloxane Precursors (Polymer-Spreying)", *J. Eu. Ceram. Soc.* (Article in Press)

[23] Schwab S. T., Blachard C. R., "The Use of Organometallic Precursors to Silicon Nitride as Binders", *Mat. Res. Soc. Symp. Proc.* Vol. 121, (1998)

[24] Lu C. C., Wei T., Pajidi A. P., "Fabrication of a SiC Fiber Reinforced Ceramic Composites by Polymer Pyrolysis Method"

[25] Suttor D., Erny T., Greil P., "Fiber Reinforced Ceramic Matrix Composites With a Polysiloxane/Boron Derived Matrix", *J. Am. Ceram. Soc.* 80 [7] (1997) 1831-1840

[26] Schmidt H., Koch D., Grathwohl G., Colombo P., "Micro/Macroporous Ceramics from Preceramic Precursors", *J. Am. Ceram. Soc.* 84 [10] (2001) 2252-55

[27] Colombo P., Hellmann J. R., Shelleman D. L., "Mechanical Properties of Silicon Oxycarbide Ceramic Foams", *J. Am. Ceram. Soc.* 84 [10] (2001) 2245-51

[28] Colombo P., Gambaryan-Roisman T., Scheffler M., Buhler P., Greil P., "Conductive Ceramic Foams from Preceramic Polymers", *J. Am. Ceram. Soc.* 84 [10] (2001) 2265-68

[29] Kotani M., Kohyama A., Katoh Y., "Development of SiC/SiC Composites by PIP in Combination with RS", *J. Nuclear Mater.* 289 (2001) 37-41

[30] Kaneko K., Kakimoto K. I., "HRTEM and ELNES Analysis of Carbosilane Derived Si-O-C Bulk Ceramics", *J. Non-cryst. Solids.* 270 (2000) 181-190

[31] Schilling C. L., JR., "Polymeric Routes to Silicon Carbide", *Brit. Polm. J.* Vol. 18, No.6 (1986) 355-358

[32] Bao X., Edirisinghe M. J., "Different Strategies for the Synthesis of Silicon Carbide-Silicon Nitride Composites from Preceramic Polymers", *Composites: Part A* 30 (1999) 601-610

[33] Wills R. R., Markle R. A., Mukherjee S. P., "Siloxanes, Silanes, and Silazanes in the Preparation of Ceramics and Glasses", *J. Am. Ceram. Soc.* (1983) 904

[34] Trassl S., Motz G., Rössler E., Ziegler G., "Characterization of the Free-Carbon Phase in Precursor Derived SiCN Ceramics", *J. Non-cryst. Solids* 293-295 (2001) 261-267

[35] Ziegler G., Richter I., Suttor D., "Fiber Reinforced Composites with Polymer Derived Matrix: Processing, Matrix Formation and Properties", *Composites: Part A.* 30 (1999) 411-417

[36] Radovanovic E., Gozzi M. F., Gonçalves M. C., Yoshida I. V. P., "Silicon Oxycarbide Glasses from Silicon Networks", *J. Non-cryst. Solids.* 248 (1999) 37-48

[37] Michalet T., Parlier M., Addad A., Duclos R., Crampon J., "Formation at Low Temperature with Low Shrinkage of Polymer/Al/$Al_2O_3$ Derived", Ceram. Int. 27 (2001) 315-319

[38] Educhi K., Zank G. A., "Silicon oxycarbide Glasses Derived from Polymer Precursors", *J. Sol-Gel Sci. Tech.* 13 (1998) 945-949

[39] Wei Q., Pippel E., Woltersdorf J., Scheffler M., Greil P., "Interfacial SiC Formation in Polysiloxane Derived Si-O-C Ceramics", *Mat. Chem. Phys.*73 (2002) 281-289

[40] Haug R., Weinmann M., Bill J., Aldinger F., "Plastic Forming of Preceramic Polymers", *J. Eu. Ceram. Soc.* 19 (1999) 1-6

[41] Baufeld B., Gu H., Wakai F., Aldinger F., “High Temperature Deformation of Precursor Derived Amorphous Si-B-C-N Ceramics”, *J. Eu. Ceram. Soc.* 19 (1999) 2797-2814

[42] www.americas.kyocera.com

[43] http://mst-online.nsu.edu/mstonline/ceramics/Table72.htm

[44] http://optoweb.fis.uniroma2.it/opto/solgel

[45] http://ceiba.cc.ntu.edu.tw/U1200/chap13/11

[46] Cahn R. W., Haasen P., Kramer E. J., “ Processing of Advanced Ceramics Part I”, *Materials Science and Technology*, Vol:17 (1996)

[47] http://www.mcelwee.net/html/densities_of_various_materials.html

[48] Walker B. E. JR., Rice R. W., Becher P. F., Bender B. A., Coblenz W. S., “Preparation and Properties of Monolithic and Composite Ceramics Produced by Polymer Pyrolysis”, *J. Am. Ceram. Soc.* No. 19-B-81 (1981)